Damage Detection of Rectangular Sections by 2D Curvelet, Contourlet and Wavelet Packet Transform

SAJAD SHAHVERDI

Abstract

In this research, the application of 2D curvelet, 2D wavelet, and Contourlet transform for damage detection of shell structure are presented. For this study, the equation of discrete curvelet transforms using unequally-spaced fast Fourier and wrapping transforms are employed. Four scenario models with one and more damages with different percentages and locations were considered for investigation of proposed methods. As real data has noise, and the existence of noise in the input data may affect the accuracy of damage detection methods. To consider the natural conditions, white noise has been applied to the data extracted from the FEM. First, the coefficients of transforms related to the noisy signal are calculated, then thresholding the previous coefficients calculated, and finally, the de-noise signal is reconstructed. Based on the presented results, the curvelet transform better identifies the location of damage than the wavelet transforms. Wavelet transform based on the direction of the damage element may be specified in some subbands. But in curvelet and Contourlet, it can better identify different damages in different directions due to the multi-directional transform. The curvelet transform has been modified based on polar space and poses challenges for non-polar (normal) discrete space. Therefore, using the Contourlet is divided into multiple directions because of each of the available general directions. According to the obtained results, the proposed methods are sensitive to the location and percentage of damage and can identify the location of damage with a low percentage of damage. Also, to confirm the results of the proposed methods, the results are evaluated using laboratory results. The results show that the proposed methods can identify the location of damages and with a percentage of damage of up to 3%.

Keywords: damage detection, curvelet transform, wavelet transform, denoising the image, contourlet transform.

1. Introduction

damage identification of structures by considering dynamic properties changes is an issue much attention has been paid to the technical literature over the past decade. The concept of damage identification means similarity of the existing structural situation of the defected material and the prior base situation that is not considered damaged.

Damage in structure probably due to any change in hardness, properties of the material, or elemental joints affected by operation forces. For instance: collision, bending, fatigue, corrosion, buckling, overstress in the time of large and unsafe structural deformations. Consequently, dynamic properties based on these changes caused some properties such as damping ratio, mode shape, and natural frequencies of the structure to deviate from the undamaged situation. Therefore, there is a need to develop advanced and robust techniques to quickly identify damages and avoid accidents that may lead to total structural rupture.

Corresponding author: E-mail address: sajad_shahverdi@yahoo.com

Damage detection methods can commonly categorize into four degrees: step 1: identification of damage in the current structure, step 2: designation of damaged geometry, step 3: Determination of the amount of damage, and step 4: Prediction of the rest of the useful life of the structure [1].

Damage identification methods can be local or global. Commonly used techniques such as magnetic fields, acoustic, eddy currents, etc., are useful but local in nature. They require that the proximity of the location of damage be easily accessible to part of the controlled structure[2]. At global methods, a structure's safety index is measured by the variation in vibratory properties[3].

Most vibration-based damage assessment methods require system detection techniques such as Fourier transform (FT) to determine the measured signals' specific characteristics. Some features of FT can affect the accuracy of damage detection. First, FT is a small process; therefore, some information about the structural condition can be lost.

Second, FT cannot show the time affiliation of signals and cannot record the changing properties typically seen in signals measured from excited structures. Structural damage is usually a local phenomenon that can be detected by prominent frequency signals. These higher frequencies generally are close together but slightly excited.

The main behavior of Fourier analysis is to transform the signal from a time or space domain into the frequency-based domain, see Figure 1. Regrettably, information concerning space or time is lost during such a transformation, and sometimes it is not possible to determine where and when a particular event occurred [3]. To remedy this deficiency, the short-term Fourier transform (STFT) was proposed by Gabor (1946)[4]. With this window technique, however, only a small portion of the signal can be analyzed at a time. The STFT explains a signal into a time-frequency or space-frequency 2D function. This future can be seen in Figure 2. The disadvantage of this progress is with reduced accuracy of space-frequency, or time-frequency information can be accrued. Higher time-frequency or space-frequency range cannot arrive simultaneously because it is similar for every frequency when the window size is selected.

The new method for exact analysis of the signal proposed is wavelet transformation (WT). The WT solves problems that other signal processing methods exhibited. Wavelet functions consist of a family of basic functions that can describe a signal in the domain of time (or space) and frequency (or scale), as shown in Figure 3.

The important advantage of using wavelets is performing local analysis of a signal, i.e., zoom in to the damaged range of time or space. The local operation application allows simultaneous modification of the time-frequency resolution, resulting in a representation with several resolutions for the transient data see Figure 3. Wavelet transform can determine hidden properties of signal that other techniques for signal analyzing cannot identify. This future is individually significant for damage identification techniques. Due to its property of multiple time-frequency resolutions, the WT has lately proven to be a useful tool for identification damage to structures.

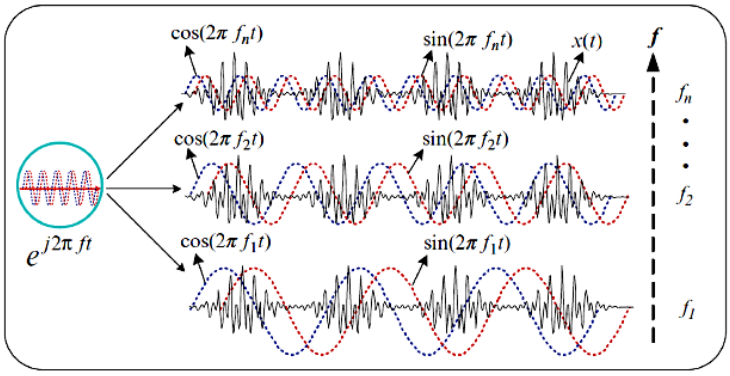

Figure 1. Fourier analysis transform [5].

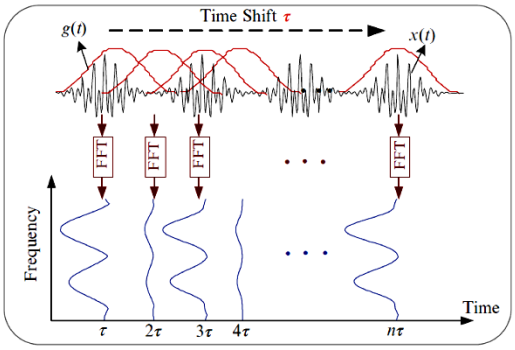

Figure 2. Application of the Short-Time Fourier Transform (STFT)[5].

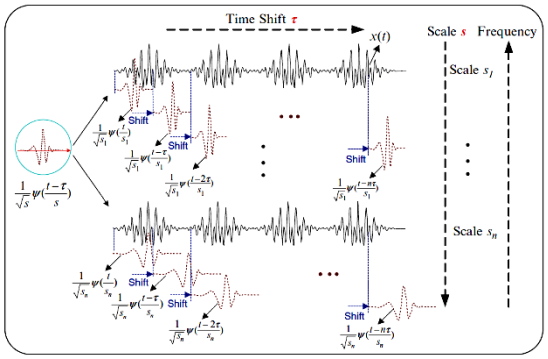

Figure 3. Demonstration on how to use wavelet transform (WT) [5].

A plausible disadvantage of WT related to the frequency resolution in the upper frequency range is relatively poor. Accordingly, discrimination is, however, difficult when it involves high-frequency components of contiguous signals. The Wavelet Packet Transform (WPT) is an extended wavelet that provides a complete signal level breakdown. The WPT is created by a linear combination of ordinary wavelet functions[6], [7]. Therefore, packet wavelet transform provides the ability to extract the characteristics of non-stationary and stationary signals at different frequencies.

The recent multi-scale power tool with the facts of all positions and directions on each needle-shaped element and scale on the fine-scale proposed is the curvelet transform. The curvelet transform shows a better performance than the traditional transforms, the same as a wavelet.

Curvelet was first introduced in 2000 by Candes and Dunho [8]. These performances are leaning the basic design, which uses a preprocessing level that includes a particular dividing of phase space pursued with transform named

Ridgelet that applied to blocks of localized data in frequency and space. Candes and Donoho presented a recent narrow curvelet frame and demonstrated that curvelets offer the optimal and most sparse image of objects with uniqueness along the C-ridges.

Man and Plonka have done a lot of research on curvelet transform. For example, they studied the application of curvelet in turbulent flows, image processing, seismic data processing, and compacted measurement. Also, they described how to use curvelet transform[9]. Ma and Plonka also review the curvelet history, including its past of wavelet transform, its reasonable connection to other multi-directional and multi-resolution methods, essential theory and separate algorithms, and the latest usage in engineering [10]. Wavelet packet energy ratio index (WPERI) proposed by Shahverdi et al. for identification of damage in free span pipeline and offshore jacket platforms [11], [12]. Lotfollahi-Yaghin and Koohdragh have also examined the performance of wavelet packet translation and continuous wavelet transformation (CWT) to identify crack properties [13]. As a result, WPT makes it possible to extract characteristics from signals that combine stationary and unstable characteristics at the damaged frequency. All of the above posts worked with frequency or time domain. Few studies have been done to identify damage to free-standing pipe structures. No one has used time-to-frequency wavelet packet translation to determine damage to these structures under ambient load (sinusoidal load). Asgarian et al. predicted the location of the damaged members of the jacket offshore platform by changing the strain energy of the elements. Damage often reduces the stiffness in some elements, hence the modal parameters; Modal shapes and natural frequencies of the damaged structure are different from those of a healthy structure. The location of the damage is determined by calculating the modal strain energy change index (MSECR) for each structural element, which elements with a higher MSECR are suspected of being damaged. For each suspected damaged element, by calculating the strain energy of the diagonal matrix (CMSE), assuming that the mass matrix of the damaged structure and the healthy structure are the same, the severity of the damage as a stiffness reduction factor - which represents the ratio of changes in stiffness to stiffness. Defective is estimated. The results show that the proposed method can be used to detect damage to these types of structures[1].

Karami et al. Investigated a method to locate multiple lesions in the beds of a dolphin jetty. In the first step of the proposed method, a damage index is introduced based on a combination of Wavelet Bundle Energy Curvature Difference (WPECD) and Richardson extrapolation, in order to precisely localize the damaged areas. Damaged piles at Dolphin Wharf. The difference in curvature of the energy of the closed wave results from the vibration signals of the structure. Using an image processing technique, in the second step of the process, the damaged areas were extracted by the WPECD process. Numerical and experimental results confirmed the effectiveness and capacity of the proposed method. A 3D scanner first scanned the exact geometry of the damage in the test model. The scanned images were then processed and entered as input files into the digital model. Finally, the results showed that the proposed method makes it possible to capture multiple structural damage with acceptable precision.[14].

Dost Mohammadi et al. Had examined the properties of voltage and current signals extracted with 2D DWT. 2D DWT can provide valuable discrete wavelet transform (DWT) functionality with a lower degree of decomposition. 2D DWT can even compress data suitable for smart grids, where large amounts of data are a problem. A new feature selection method has been proposed to reduce redundant data, feature vector dimensions, and computational load. The selector backbone is the classification function used in the corresponding pattern system and compatible with the classification.

The results show the high precision of the proposed method to identify the factors that cause vibrations in VAWTs. It has been shown that the characteristics extracted from the current and voltage signal by 2D DWT are superior to the characteristics extracted from the voltage signal by DWT. He also demonstrated the advantage of selecting the proposed functionality over the Relieff method[15]. Nigam and Singh investigated that an optimistic attempt to detect cracks in a ray using a discrete wavelet transform has been proposed. The finite element beam model is considered to be simply supported with transverse open cracks. The tearing of a beam causes a discontinuity in the slope in the elastic line. The beam deflection is used to determine the location of the slope discontinuities using the wavelet transform. The effect of the noise measured on the surface of the wavelet decomposition was examined. For experimental research, an inexpensive method based on the digital image was used to obtain a deflection of the cracked beam. White pixels are removed due to dust particles using the component algorithm. An appropriate edge detection technique is selected to find the edge image based on the signal-to-noise ratio values. The edgeless deflection of the beam is used as an input to convert the wavelet to detect the location of the crack. The detection of cracks in beams with different crack depths was investigated experimentally. The proposed method works well with simulated and experimentally measured crack deformations. [16]. Yan and Yam were identified using wavelet analysis on composite panels to analyze dynamic responses[17]. Ashory et al. had investigated the introduction of a combined damaged detection method, which both increases the sensitivity of damaged detection and detects quantitative parameters of injuries. The wavelet transformation determines the location of the initial damage, and the damage parameters, including location, depth, and severity, were separated during the model update process. The wavelet transform is obtained as a function of the nature of the signals, which results in better wavelet transform performance. Then the elevator design algorithm process was performed to increase the efficiency of the wavelets in damage detection. In addition, an appropriate signal based on the strain energy was used to detect wavelet transform damage. Finally, the genetic algorithm method was used in the proposed model update method to identify the damage parameters using a new error function. The selected error function was based on strain energy and had the best performance among the previously defined criteria. Consequently, the precision of the identification of the damage parameters using the proposed method has been improved, especially in the presence of noise. Additionally, this solution is faster than previous update methods which only used genetic algorithms based on naturally occurring shapes and frequencies to detect damage. [18]. Poodle et al. Suggested using digital video images to see damage in structures. Mode shapes are derived from time series to determine the functions of the state difference function between damaged and reference modes. They were subjected to a wavelet transform in order to determine the location of the damaged[19].

Hajizadeh et al. Focused on damage detection of various types of faults in plate structures using wavelet transform (WT) and curvelet translation (CT). These two methods have been further developed to diagnose injury in the last few years. In recent years, the Curvelet transform method has been introduced to overcome the inherent limitations of traditional multiscale transformations such as wavelets. In this study, the performance of curvelet and wavelet transforms is compared in order to demonstrate their ability to detect various types of faults in plate structures. This goal is investigated by causing various types of damage to the rectangular sheet that is trapped on all four sides. Using the first model of the plate structure and distributing the coefficients of variation, the presence of damage, the location of the failure and the approximate shape of the failure are identified. In addition, the accuracy and performance of the

transformations are confirmed by the use of one-page modal experimental data[20]. Bagheri et al. Have studied a new method based on Curvelet translation to evaluate the position of damage in plate structures. In this study, Curvelet was used to identify linear properties due to its optimal performance. Discrete Curvelet translation equations were investigated using Fourier transform fast to detect plate damage. The proposed method is investigated using a rectangular plate containing one or two faults of damaged length, depth and location. After that, damage to the plate was detected using the proposed method. By comparing the situation obtained from the proposed method and the simulated model, they found that the proposed method is sensitive to damage. In addition, the performance of the method has been confirmed through the use of experimental data [21].

In the study of Ying et al., The first discrete three-dimensional curvelet transform is presented. This conversion is a format for translation two-dimensional curvelet provided by Candes et al[22][23]. Rucka and Wilde proposed a method to estimate the location of the damage in the beam and in the plate using a continuous wavelet transform, the location of which is determined by a peak in the spatial variation of the transformed response[24]. Bayissa et al. proposed damage identification technique using the continuous wavelet transform to detect damage in a concrete plate model and in steel plate girder of a bridge structure[25].

2. Wavelet Analysis

The wavelet transforms as a development of the traditional Fourier transform method that can provide a time-frequency analysis and multi-resolution analysis of non-stationary data.

This method can identify d structures' damage according to previous research [26]. In this research, the application of wavelet transform method in two-dimensional structures is investigated. Below is a brief description of the equations of this method.

Wavelet is a function $\Psi(x) \in L^2(R)$ that is an oscillatory, real or complex value with finite length and zero mean[13]. The mother wavelet 'ψ (x) ', that is the fundamental wavelet function, is dilated (compressed or stretched) by s and translated in space by τ to generate a set of basic functions $\Psi_{s\tau}(x)$ as follows [13]:

$$\Psi_{s,\tau}(x) = \frac{1}{\sqrt{s}}\Psi\left(\frac{x-\tau}{s}\right) \tag{1}$$

The wavelet transform (in the version of discrete or continuous) show a connection between the function f(x), with $\Psi_{s,\tau}(x)$.

The continuous wavelet transform (CWT) coefficients is presented as follow:

$$C(s,\tau) = \frac{1}{\sqrt{s}}\int_{-\infty}^{\infty} f(x)\Psi\left(\frac{x-\tau}{s}\right)dx = \int_{-\infty}^{\infty} f(x)\Psi_{s\tau}(x)dx \tag{2}$$

The above equation (2) shows how the wavelet transform is related to the feature of signal by decomposition.

Therefore, high-amplitude wavelet coefficients indicate the existence of strong transitions in f(x), which is exactly the basis of the damage identifying method of f(x).

For constructing the main function $f(x)$ from its wavelet coefficients C (s,τ), we need inverse function.

Then, the CWT has an inverse that is defined by retrieving the coefficients C from the wavelet transform to $f(x)$ according to the following equation;

$$f(x)=\frac{1}{K_{\Psi}}\int_{s=-\infty}^{s=\infty}\int_{b=-\infty}^{b=\infty}C(s,\tau)\Psi_{s\tau}(x)d\tau\frac{ds}{s^2} \tag{3}$$

The value of K_{ψ} depends on the type of wavelet. Generating of large number of wavelet coefficients during decomposition is one of the main drawbacks of CWT transform [27]. As previous research has shown, all of CWT coefficients (C(s,τ)) are not required to reconstruct the $f(x)$, and some of them based on the purpose of translation, that are not necessary can be omitted[13]. Therefore, the parameters' discrete values are used instead of using the continuous wavelet transform [27]. Discrete Wavelet Transform (DWT) can be defined using discrete scales; for more details, please refer to [27]:

$$C_{j,k}=\frac{1}{\sqrt{2^j}}\int_{-\infty}^{\infty}f(x)\Psi(\frac{x-k2^j}{2^j})dx=\int_{-\infty}^{\infty}f(x)\Psi_{j,k}(x)dx \tag{4}$$

The inverse of the scale $\frac{1}{s}=2^j$ represented the resolution of the signal and the level of decomposition is presented by the integer of j.

Decreasing the level and scale increases the resolution and allows finer and smaller parts of the function $f(x)$ to be gained access.

Like a CWT, the signal can be reconstructed from the wavelet coefficients $C_{j,k}$, and the reconstruction algorithm is called an Inverted Discrete Wavelet Transform (IDWT).

$$f(x)=\sum_{k=-\infty}^{\infty}c_{j,k}\psi(2^{-j}x-k)\sum_{j=-\infty}^{\infty}\frac{1}{2^{j/2}}. \tag{5}$$

replacing ϕ(x) insisted of ψ (x) in equation (2) function D (s0, τ) can be obtained as follow:

$$D(s_0,\tau)=\int_{-\infty}^{\infty}\frac{1}{\sqrt{s_0}}\phi(\frac{x-\tau}{s_0})f(x)dx=\int_{-\infty}^{\infty}f(x)\phi_{s_0,\tau}(x)dx \tag{6}$$

According to the following equation, the coefficients are obtained by applying equation (4) following this equation.

$$cD_J(k)=\int_{-\infty}^{\infty}f(x)\Psi_{j,k}(x)dx \tag{7}$$

The coefficients $cD_J(k)$ expressed in eq. (7) are known as the detail coefficients at J-level of decomposition.

Using the binary scale and the decomposition level of J, eq. (6) leads to a series of other coefficients as follows:

$$cA_J(k)=\int_{-\infty}^{\infty}f(x)\phi_{J,k}(x)dx \tag{8}$$

The coefficients $cD_J(k)$ expressed in eq. (8) are known as the approximation coefficients at J-level of decomposition.

Then by applying the inverse of wavelet transform to the approximation and detail coefficients, as bellow the f(x) reconstructed:

$$f(x)=\sum_{j=-\infty}^{\infty}\left(\sum_{k=-\infty}^{\infty} cD_j(k)\psi_{j,k}(x)\right)+\sum_{j=-\infty}^{\infty} cA_J(k)\phi_{j,k}(x). \tag{9}$$

The function stated above (eq. (9)) is divided into two parts. The part in the parentheses is known as the detail function at the decomposition level j, which is expressed by the following equation:

$$f(x)=\sum_{k=-\infty}^{\infty} cD_j(k)\psi_{j,k}(x) \tag{10}$$

The second part of eq. (9) is called the approximation function at the J level of decomposition:

$$A_J(x)=\sum_{j=-\infty}^{\infty} cA_J(k)\phi_{j,k}(x). \tag{11}$$

As shown in Eq. (9) and figure 5, the main performance of the wavelet transform can be understood as the sum of the approximation coefficients of the decomposition plus all the coefficients of the decomposition details up to the same level:

$$f(x)=A_J(x)+\sum_{j\le J} D_j(x). \tag{12}$$

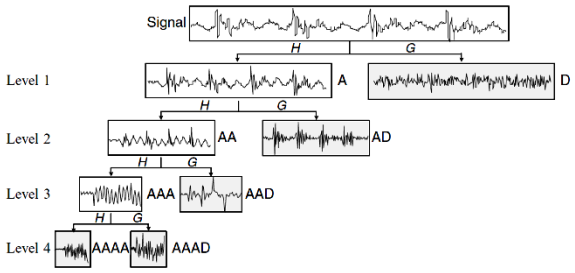

Figure 4. Discrete Wavelet Transform Decomposition Tree

To using wavelet transform in any type of application, the most important case is to use the most appropriate type of wavelet for the damaged transform. In this study, to analyze the structural models, the optimal wave has been selected using trial and error.

3. Wavelet Packet Transform

Using DWT analysis by applying a binary filter bank, only the approximation components at each level of the analysis are obtained, which results in low-frequency resolution at low levels such as A1 and D1.

Therefore, it may cause problems when using DWT where vital information is in the higher frequency components. To solve this problem, wavelet packet translation (WPT) is proposed. WPT is similar to DWT, except that in addition to decomposing only the approximation component at each level, a component is further decomposed to obtain its own approximation components and details. To see how the wavelet packet transform works see Figure 5.

The WPT has the feature such as time-frequency localization and orthonormality. Providing that the wavelet packet functions are orthogonal

$$\psi_{j,k}^{m}(t)\psi_{j,k}^{n}(t)=0 \qquad \text{if } m\neq n \tag{13}$$

WPT $\psi_{j,k}^{i}$ is a function expressed in the following equation with three indices in which the integers k,j and i are the translation, scale, and modulation parameters, respectively.

$$\psi_{j,k}^{i}=2^{j/2}*\psi^{j}(2^{j/2}t-k), \quad i=1,2,3,... \tag{14}$$

By applying WPT to function $f(t)$ the $c_{j,k}^{i}(t)$ WP coefficients obtained as bellow:

$$c_{j,k}^{i}(t)=\int_{-\infty}^{\infty} f(t)\psi_{j,k}^{i}(t)dt, \tag{15}$$

The signal $f_{j}^{i}(t)$ can be demonstrated by eq. (16) that is a combination of wavelet packet functions $\psi_{j,k}^{i}(t)$:

$$f_{j}^{i}(t)=\sum_{i=1}^{2^{j}} c_{j,k}^{i}(t)\psi_{j,k}^{i}(t), \tag{16}$$

the original signal f(t) after decomposition of signal with WPT at j level, can be represented as:

$$f(t)=\sum_{i=1}^{2^{j}} f_{j}^{i}(t), \tag{17}$$

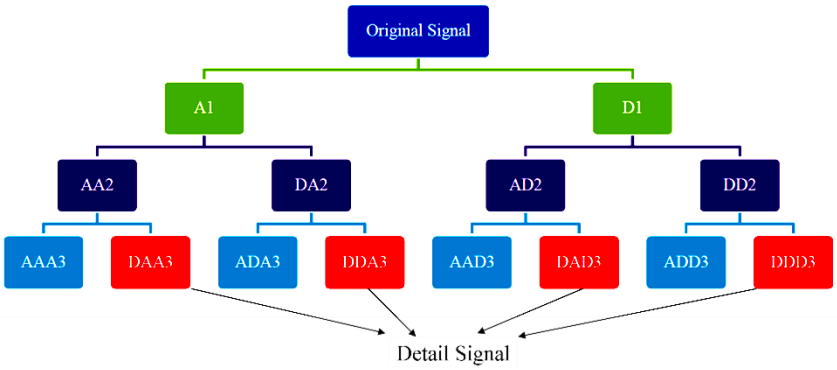

Figure 5. The tree of WPT Decomposition [11], [28]

4. Methodology

4.1. 2D Wavelet transform

4.1.1. 2-D discrete wavelet transform

Considering that multi-resolution analysis theories are presented in one dimension, but most of the problems required by the engineering department are two-dimensional and three-dimensional. Therefore, these theories can be generalized to higher dimensions, for example, as (18):

$$\varphi(x,y)=\varphi(x)\varphi(y) \tag{18}$$

in the following equation, we will have expansion by applying the dilation conditions:

$$\varphi(x,y) = 2\sum_{k,l} h(k,l)\varphi(2x-k, 2y-l) \tag{19}$$

As mentioned above, most of the engineering data is two-dimensional. Therefore, the two-dimensional wavelet transform developed based on a one-dimensional wavelet is used to analyze them. The two-dimensional wavelet is the combination of three decomposed matrices of horizontal, vertical, and diagonal coefficients [21]:

$$\begin{aligned} \psi^V(y,x) &= \psi(y)\varphi(x) \\ \psi^H(y,x) &= \varphi(y)\psi(x) \\ \psi^D(y,x) &= \psi(y)\psi(x) \end{aligned} \tag{20}$$

Where $\psi^V, \psi^H \; and \; \psi^D$ measures variations along with columns, rows, and diagonals coefficients. The one-level 2D wavelet decomposition shows in Figure 6. For other levels of decomposition can be obtained shows a one-level decomposition. The other levels of decomposition are obtained by repeating the above decomposition on the low-pass image aa.

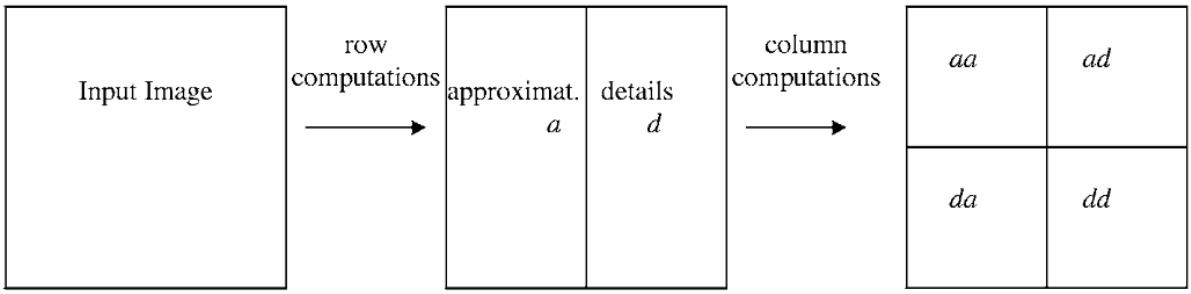

Figure 6. Schematic diagram of the input image in the first level using two-dimensional wavelet transform

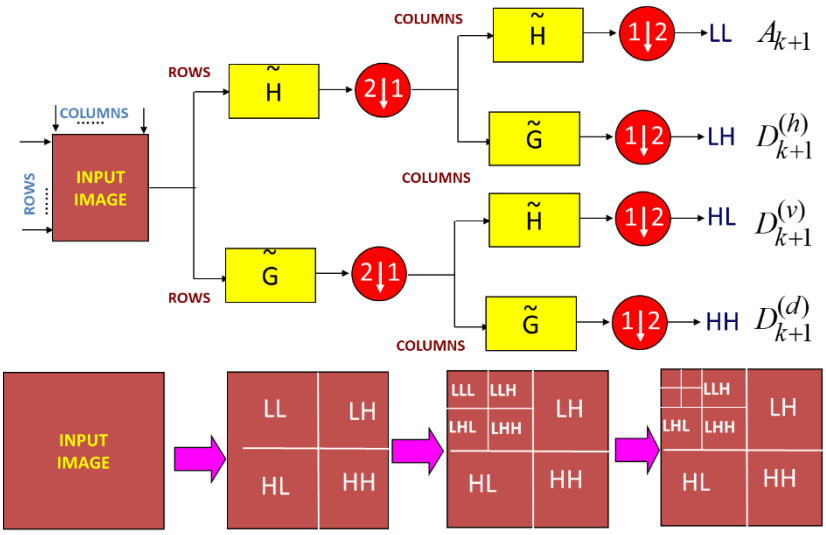

Figure 7. Algorithm of decomposition of the input image by using 2-D wavelet transform

4.2. Curvelet 2D transform

The new design of curvelets transform is in the form of two-dimensional waveforms presented for multidimensional analysis in two-dimensional space.

Like wavelets, curves can be localized in scale (frequency domain) and position (spatial domain). Still, the advantage of using them is the localized orientation that is not present in wavelets. This feature of the curvelets provides the curved structure with interesting features; this feature is a completely scattered description of the uniqueness's based on the C^2 curves aboard two dimensions. In the spatial dimension, a j-scale curvelet is a directional weight that is enclosed in a rectangle measuring 2^{-j} by $2^{-j/2}$ and thus follows the ratio of the width ≈ length2. In the frequency dimension, a j-scale curvelet is a wedge whose frequency coverage is inside a rectangle measuring 2j by 2j/2.

It is a dispersed optimized base for Fourier integral operators (FIOs), Pseudo-differential operators (PDOs), and for several problems of image processing can be a useful tool.

4.2.1. Continues curvelet transform

In this section, we introduce the equation of curvelet transform in two-dimensional space. Suppose $x = (x_1, x_2)$ is the location variable, ω is the frequency variable, and r and θ are the polar coordinates of the frequency space. Also, consider the two variables W(r) and V (t), with the names of the radial and angular windows, respectively. These two are uniform, non-negative, and with real values.

The amplitude of the function W positive numbers belongs to the interval r ∈ [3/4, 3/2] and the amplitude of the function V of the real numbers belongs to the interval t ∈ [-1/2, 1/2]. Besides, these two window functions always follow the following conditions:

$$\sum_{j=-\infty}^{j=+\infty} W^2(2^j r) = 1 \quad r \in (3/4,3/2\,) \tag{21}$$

$$\sum_{l=-\infty}^{\infty} V^2(t-l) = 1 \quad r \in (-1/2,1/2\,) \tag{22}$$

Now using these two equations, the frequency window defined in Fourier space for each j ≥ j_0 the as follows:

$$U_j(r,\theta) = 2^{-\frac{3j}{4}} W(2^{-j}r) V(\frac{2^{\lceil \frac{j}{2} \rceil}\theta}{2\pi}) \tag{23}$$

Where (j/2) represents the integer part of *j/2*. Thus, the definition of the domain U_j is a polar parabolic wedge that is applied by W and V to scale-dependent extensions in different directions. To obtain real-valued curvelets, it is easy to work on the symmetrized of, $U_j(r,\theta) + U_j(r,\theta+\pi)$.

In this equation, we will introduce the mother of curvelet $\varphi_j(x)$ with scale j, the reason for this naming is that curvelets with scales 2^{-j} are obtained by rotation or transfer of $\varphi_j(x)$. Consider the following two definitions:

- Equal set of distances of the angles of the period $\theta_l = 2\pi.2^{-\lceil \frac{j}{2} \rceil}.l$ with $l = 0,1,..$ Such that $0 \le \theta_l < 2\pi$ (note that the distance between two consecutive angles depends on the scale).
- and set of transfer parameters $k = (k_1, k_2) \in Z^2$.

Using these definitions, curvelets with 2^{-j} scale and function of $x = (x_1, x_2)$, position $x_k^{(j,l)} = R_{\theta_l}^{-1}(k_1.2^{-j}, k_2.2^{-j/2})$ and orientation θ_l can be created as follows:

$$\varphi_{j,l,k}(x) = \varphi_j\left(R_{\theta_l}\left(x - x_k^{(j,l)}\right)\right), \tag{24}$$

Where R_θ is the radius θ angle, and R_θ^{-1} its inverse (also its transpose);

$$R_\theta = \begin{pmatrix} cos\theta & sin\theta \\ -sin\theta & cos\theta \end{pmatrix}, R_\theta^{-1} = R_\theta^T = R_{-\theta}. \tag{25}$$

the curvelet coefficients are simply obtained by the internal multiplication of the elements $f \in L^2(R^2)$ and $\varphi_{j,l,k}$,

$$c(j,l,k) = < f, \varphi_{j,l,k} > = \int_{R^2} f(x).\bar{\varphi}_{j,l,k}(x)dx. \tag{26}$$

Like what we have about wavelet transform, there are large-scale elements in the curvelet pyramid. For $k_1, k_2 \in Z$, large-scale curvelets are defined as follows:

$$\varphi_{j_0,k}(x) = \varphi_{j_0}(x - 2^{-j_0}k) \tag{27}$$

$$\widehat{\varphi}_{j_0}(\omega) = 2^{-j_0} W_0(2^{-j_0}|\omega|) \tag{28}$$

Thus, curvelet with all scale transforms include directional elements $(\varphi_{j,l,k}), j \ge j_0, l, k$ on a small scale and isotropic wavelets on a large scale. Figure 8 summarizes the main components of a curvelet.

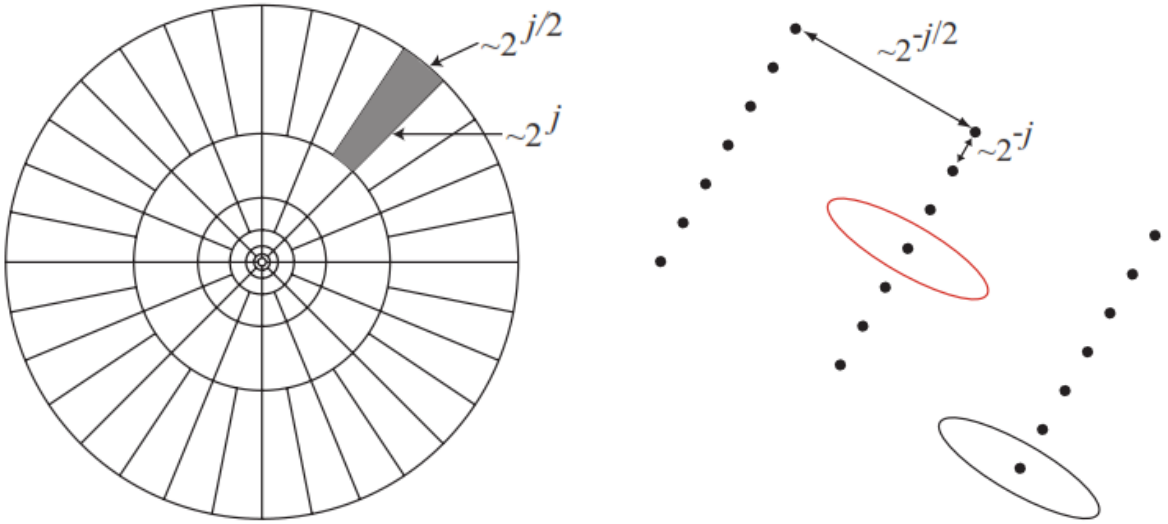

a) b)

Figure 8: The basic explanation of digital tiling (frequency and space). Figure a, shows the induced tiling of the frequency space separation. The figure b, shows symbolically expresses the Cartesian network of space of a particular scale and direction [23].

4.2.2. Discrete curvelet transform

The Collection of cartesian curvelets for discrete curvelet transform (DCT) suggested [22], [23]. The important components key of this construction summarized in **Error! Reference source not found.**.

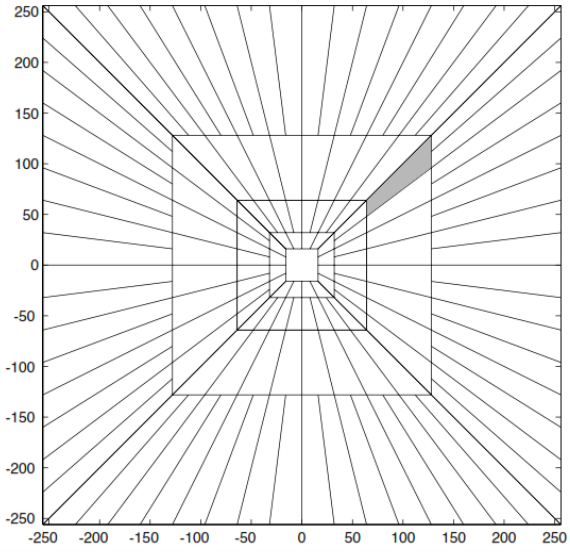

Figure 9:shows the basic digital tile of the image. The windows $\widetilde{U}_{j,l}$ gently place the Fourier transform near the obedient parabolic scale wedges. The shaded area represents such a typical wedge [23].

$$\tilde{\varphi}_{j,l,k}\ \ (x) = 2^{\frac{3j}{4}}\tilde{\varphi}_{j,}(R_{\theta_l}^{T}(x - R_{\theta_l}^{-T}b) \tag{29}$$

Where $\mathrm{b} = (k_1.2^{-j}, k_2.2^{-j/2})$ and $\mathrm{R}_\theta = \begin{pmatrix} cos\theta & sin\theta \\ -sin\theta & cos\theta \end{pmatrix}, R_\theta^{-1} = R_\theta^T = R_{-\theta}$

$$\mathrm{R}_\theta = \begin{pmatrix} 1 & 0 \\ -\tan\theta & 1 \end{pmatrix} \tag{30}$$

the discrete curvelet coefficients given:

$$C(j,l,k) = \frac{1}{(2\pi)^2}\int (\hat{f}(\omega)\widetilde{U}_j R_{\theta_l}^{-1}\omega) e^{i\langle R_{\theta_l}^{-T}\mathrm{b},w\rangle}\, d_\omega = \frac{1}{(2\pi)^2}\int \hat{f}(\mathrm{R}_\theta\omega)\widetilde{U}_j(\omega)\, e^{i\langle \mathrm{b},w\rangle} d\omega \tag{31}$$

Where $\widetilde{U}_j(\omega)$ is cartesian window based on bellow equation ():

$$\widetilde{U}_j(\omega) := \mathrm{V}_j(\omega).\widetilde{W}_j(\omega) = V(2^{\left[\frac{j}{2}\right]}.(\omega_2/\omega_1)).\sqrt{\psi_{j+1}^2(\omega) + \psi_j^2(\omega)}$$

So that ψ is defined as a 1D low-pass window product defined:

$$\psi_j(\omega_1,\omega_2) = \varphi(2^{-j}\omega_1)\,\varphi(2^{-j}\omega_2),\ 2^j \le \omega_1 \le 2^{j+1} and\ -2^{-\frac{j}{2}} \le \frac{\omega_1}{\omega_2} / \le 2^{-j/2} \tag{32}$$

The coefficients of DCT become:

$$c^D(j,l,k) = \sum_{n_1,n_2} \hat{f}[n_1, n_2 - n_1\tan\,\theta_l]\widetilde{U}_j[n_1,n_2] e^{i2\pi(\frac{\mathrm{k}_1 n_1}{\mathrm{L}_{1,j}} + \frac{\mathrm{k}_2 n_2}{\mathrm{L}_{2,j}})} \tag{33}$$

More information can be found in Candes and Donho [23]

4.3. Contourlet transform

Contourlet's main purpose was to acquire a scattered development for ordinary 2D signals that are partially away from straight lines. 2D wavelets, with the basic functions of the tensor product as shown in Figure 10(a), are directionless and only skilled at capturing point interruptions but cannot obtain the lines' geometric strainer. Contourlets have been developed for this inefficiency as an improvement over wavelets. The resulting transformation has time-frequency in the wavelets' local and multi-scale properties and provides a high level of anisotropy and direction. In particular, as shown in Figure 10(b), the contourlet transform includes a fundamental purpose in any authority of two directions with visible appearance ratios. Together with this basic collection of functions, the smooth contour can be represented with contourlet coefficients smaller than the wavelets, as shown in Figure 11.

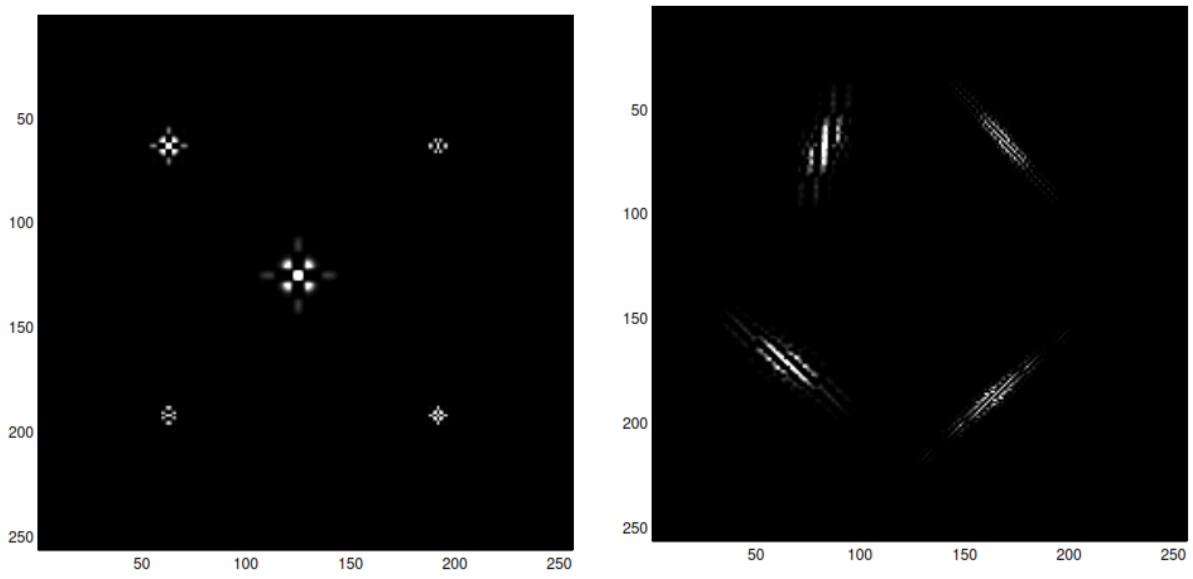

a b

Figure 10: Comparing a contourlet and wavelet display for 2D signals (images). (a) five basic wavelet images. (b) four basic contourlet images.

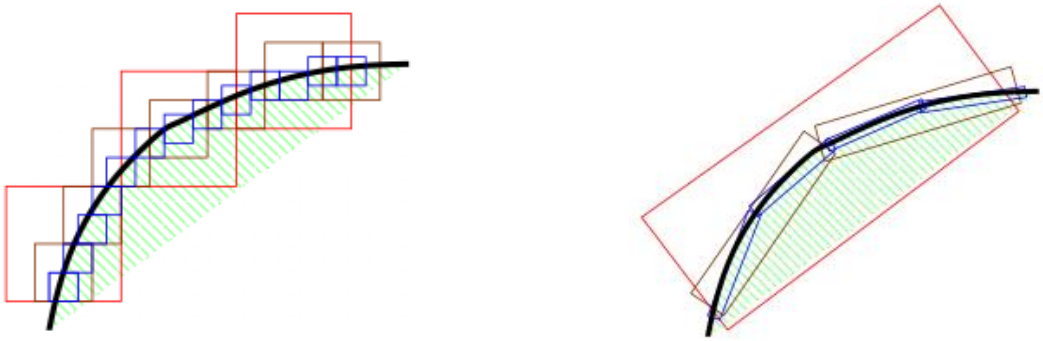

a) wavelet transform b) contourlet transform

Figure 11: An image that shows square-supported wavelets that only point interruptions can be recorded, while b) contourlet with lengthened backing can record linear sections of lines, and therefore can successfully show with lower coefficients of a smooth contour.

Based on this structure, the multi-scale cascade and the directional analysis decomposition steps at the CT are independent. Each scale can be decomposed to any damaged value from two directions, and various scales can be decomposed into different directions. This feature causes the CT a special transform that can reach a brilliant variability in decomposition while close to critical sampling (till 33% too full, which achieve from the LP).

This transform, as shown in Figure 12, is based on Laplace Pyramid (LP) filter bank and directional filter bank (DFB), which constructed a Pyramid Directional Filter Bank (PDFB).

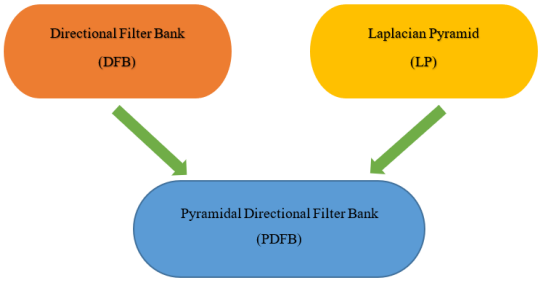

Figure 12: DFB and LP for contourlet transform

LP: Each LP stage consists of two operations:

Step 1: Reduction action, A Low Pass (LP) filter to an input signal applied then subsamples the signal multiplied by 2 in every dimension.

Step 2: Development action, the output of the previous step was upsampled by 2 in each dimension, and then the LP filter was applied to the signal.

As illustrated in Figure 13, the input signal is applied by a low pass filter (LPF) named H, then M that is the sampling matrix in each dimension of signal subsampled by 2. This produces part C, which is the approximate section of the signal (reduction action). In the next step, C is upsampled by a coefficient of 2 (sampling matrix), and then G (LPF) applies to it (expansion action). Finally, by subtracting it from the original signal, d is generated as the signal detail. Hence:

$$C = reduction\ action \tag{34}$$

$$d = signal - expand\ action \tag{35}$$

This action repeated the same on C.

DFB: A binary l-level tree decomposition of 2l subbands corresponds to 2l construction filters $D_k^{(l)}$ and a sampling matrix. Diagonal forms of sampling matrices are defined as the following equation:

$$S_k^{(l)} = f(x) = \begin{cases} dia(2^{l-1}, 2) & 0 \le k < 2^{l-1} \\ dia(2, 2^{l-1}) & 2^{l-1} \le k < 2^l \end{cases} \tag{36}$$

The sampling matrices consist of two parts: mostly horizontally based on $0 \le k < 2^l$ also mostly vertical based on $2^{l-1} \le k < 2^l$.

PDFB: Suppose it $a_0[n]$ represents the input image, then the l-level of the Laplace Pyramid breaks down the image $a_{j-1}[n]$ into a rough (bandpass) image and a detailed image $b_j[n]$. Besides, the lj-level directional filter bank decomposed each $b_j[n]$ into the 2^{l_j} bandpass directional images. Then, with applying lj-level DFB decomposition on $b_j[n]$, CT coefficients would be presented as:

$$c_{j,k}^{(l_j)} = S, \lambda_{L+j,k,n}^{l_j} \tag{37}$$

Which $c_{j,k}^{(l_j)}$ is CT coefficients at scale L, j=1,2, 3, …, j.

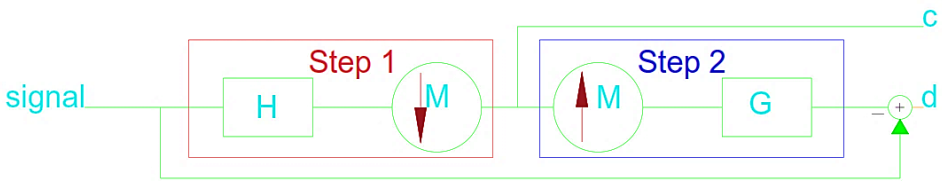

Figure 13: Laplace Pyramid decomposition; c

5. Damage identification method

This article aims to introduce the method according to the Curvelet transformation to identify different damage shapes in rectangle structures. In the suggested transform, by using FFT the discrete curvelet transform is computed that are unevenly spaced.

5.1. Mode shape estimation

Numerical models are developed as a rectangular plate in both states of the structure with damage and without damage in ANSYS finite element software. The input data of the damaged translation used for damage detection is extracted based on the structure's displacements due to its shape and uniform load on the structure.

The geometric shape of the damaged rectangular plate is generally shown in Figure 14.

As shown in Figure 14, the damaged area's dimensions and size are generally equal to the B*L*t and D*w, respectively. Also, the damage location is at a distance of L1, B1 from the left corner of the plate and with an angle of α. The damaged part is expressed by decreasing in thickness or modulus of elasticity. The free vibration equation for a damaged structure is defined as follows:

$$M\ddot{X} + C\dot{X} + KX = 0 \tag{38}$$

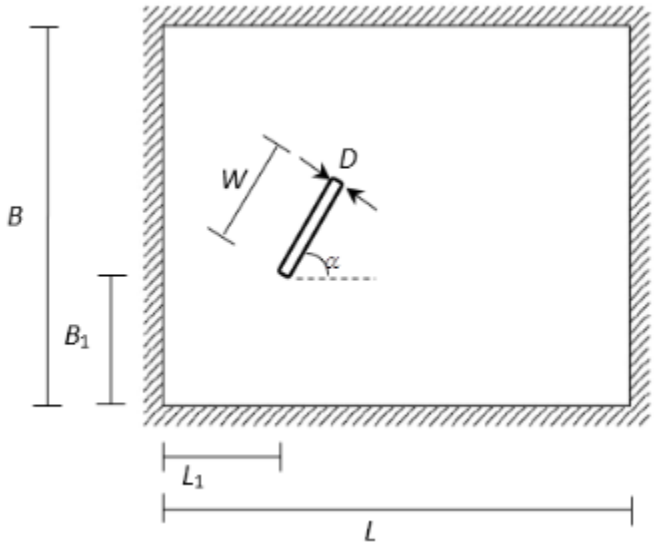

Figure 14: damage location and geometry of the structure

where K, C, and M are stiffness, damping, and mass matrices, respectively. Mode shapes are obtained by solving the above equation. In this study, in addition to using the structure's mode shape, static analysis of the structure under the effect of uniform load on the plate has been used. Solving Equation (38) leads to calculating of the mode shape, which i, is the number of mode shapes. In cases related to damage diagnosis, in addition to using the mode shape, the displacement of the structure in both damaged δ^d and healthy modes δ^u can be used.

Damage of structure is modeled by defining Young modulus degradation or thickness reduction or any change that leads to a change in the dynamic behavior of the structure. For example, the following equation shows how to calculate the Young's modulus of the damaged structure:

$$E^d = E(1-d) \tag{39}$$

Where E and E^d are the undamaged and damaged modulus of Young's, respectively, and the intensity of element damage is d in the finite element model.

5.2. Apply noise to data and denoising input data

The input data extracted from the real structure include noise. The existence of noise may have a significant effect on the damage detection accuracy. Noise reduction is one of the unavoidable, important of damage identification. One problem is knowing it is not predestined with assurances of how much and whether the data measured are distorted with the noise. If denoising methods are improperly applied to very low-noisy data, useful future information important to damage identification may be wasted from this process, leading to incorrect results [21], [29].

For the application of data denoising based on the curvelet transformation, Bagheri et al. proposed three steps as below [21], [30]:

- Recording data from the finite element method (FEM),
- Apply the noise to the data (simulate the actual data),
- Calculate the xlet-based decomposition of data contain noise,
- The threshold value of coefficients computed,
- Then the denoising data reconstructed.

In this section, the curvelet transform is used to remove noise from the extracted data of the structure. The standard method is used to delete extra data. Suppose the data containing the noise are obtained as follows:

$$\delta^n = \delta(1+\eta\Delta) \tag{40}$$

Where η and Δ are the degree of noise and random matrix in the range of [-1,1], respectively.

5.3. Calculation of damage index

To determine the damaged transforms coefficients based on mode shape, discrete curvelet transform based on the wrapping method is used. The i^{th} transform coefficients for damaged and healthy structures are c_i^d and c_i^u, respectively Finally, the damage detection index is calculated based on the relative root mean square error of the damaged and healthy structural coefficients for the i^{th} node, and as a result, the damage index is defined as follows:

$$c^m(j,l,k)_i = c_j^d - c_j^u \quad \text{j=1, 2, …, n.} \tag{42}$$

Where n is number of input image nodes. Denoising is achieved using a hard threshold law for estimating unknown curvelet coefficients [18]. There are many methods for calculating the noise level, for example, by calculating the norm of a unique curvelet, and in this paper, we use the forward curve to form a state with a delta function at its center. Finally, the denoised mode shape was obtained based on the inverse curvelet deformation.

According to Table 1, the proposed methods for damage identification using 4 scenarios with different damage, as well as with different length, width and position are shown.

Table 1: scenario type and damaged percentage

Scenario	Type of Damage	Damage percentage
1	Tow triangular damaged shapes	reduced 5% of the thickness
2	one triangular damaged shape	reduced 5% of the thickness
3	Tow rectangular damaged shapes	reduced 3% of the thickness
4	One oblique damaged shape	reduced 3% of the thickness

For this purpose, four scenarios as bellow conceded:

Scenario 1: a fixed support rectangle structure considered with 600 cm width, the thickness 200 mm, and 600 cm height. The material properties of the rectangle structure are assumed to include Young's modulus E = 20 GPa, the mass density of ρ=2500 kg/m, and Poisson's ratio $\vartheta = 0.3$. ANSYS WORKBENCH software package has been employed to build the model used in the finite element method. In the finite element model, the damage is represented as the elements with the reduced thickness or Young's modulus. To damage detection, two damage triangles have been considered. The FEM model is shown in Figure 15.

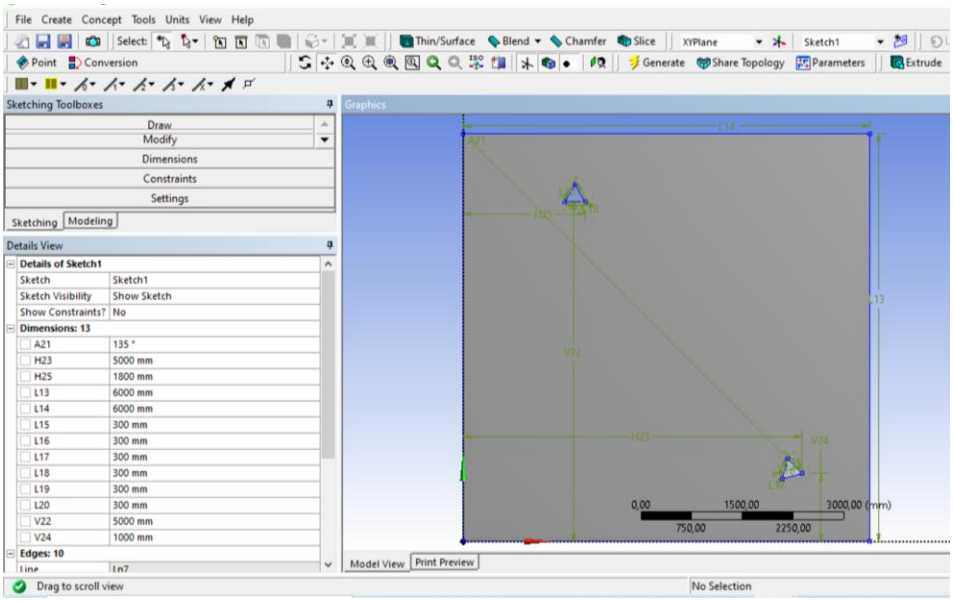

Figure 15: scenario 1, Geometry of the rectangle structure was considered triangular damage with 5 percent reduced thickness.

As shown in **Error! Reference source not found.**-a, the FEM model meshed, Figure 16(b) the noise data added to the input data for simulation of reality situation, and the first mode shape of the damaged and undamaged model was used as input data for proposed methods Figure 16(c,d). Figure 17 shows the application of 2D wavelet transform. According to the figure shown, depending on the damage's direction, each of the sub-bands may show a part of the damage location. For example, horizontal wavelet coefficients can detect only damage in the horizontal direction as Figure 17(b), vertical wavelet coefficients are only able to show vertical damage as Figure 17 (c), and also diagonal wavelet coefficients show only diagonal damage as Figure 17(d), and this is a sign of one-way wavelet. This shows the weakness of the above method, and therefore two-dimensional curvelet has been used to identify the damage, the results shown in Figure 18.

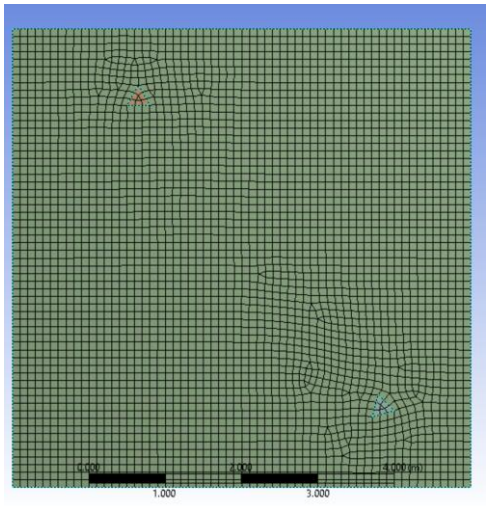

a

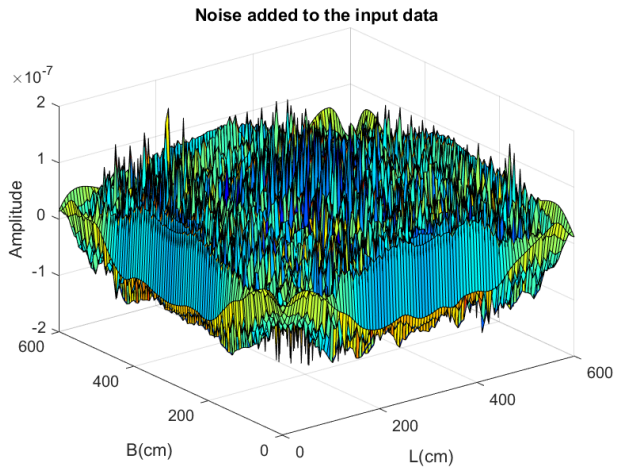

b

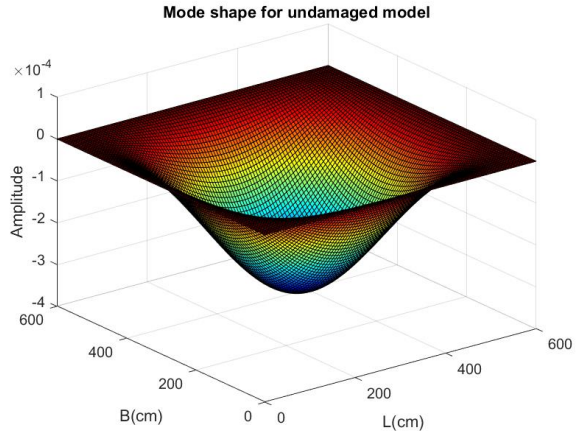

c

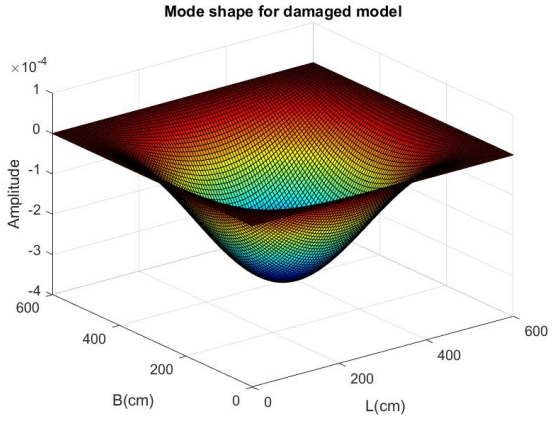

d

Figure 16: a) FEM model meshed of scenario 1, b) Noise added to input data (random), c) Mode shape of undamaged model, and d) mode shape of damaged model

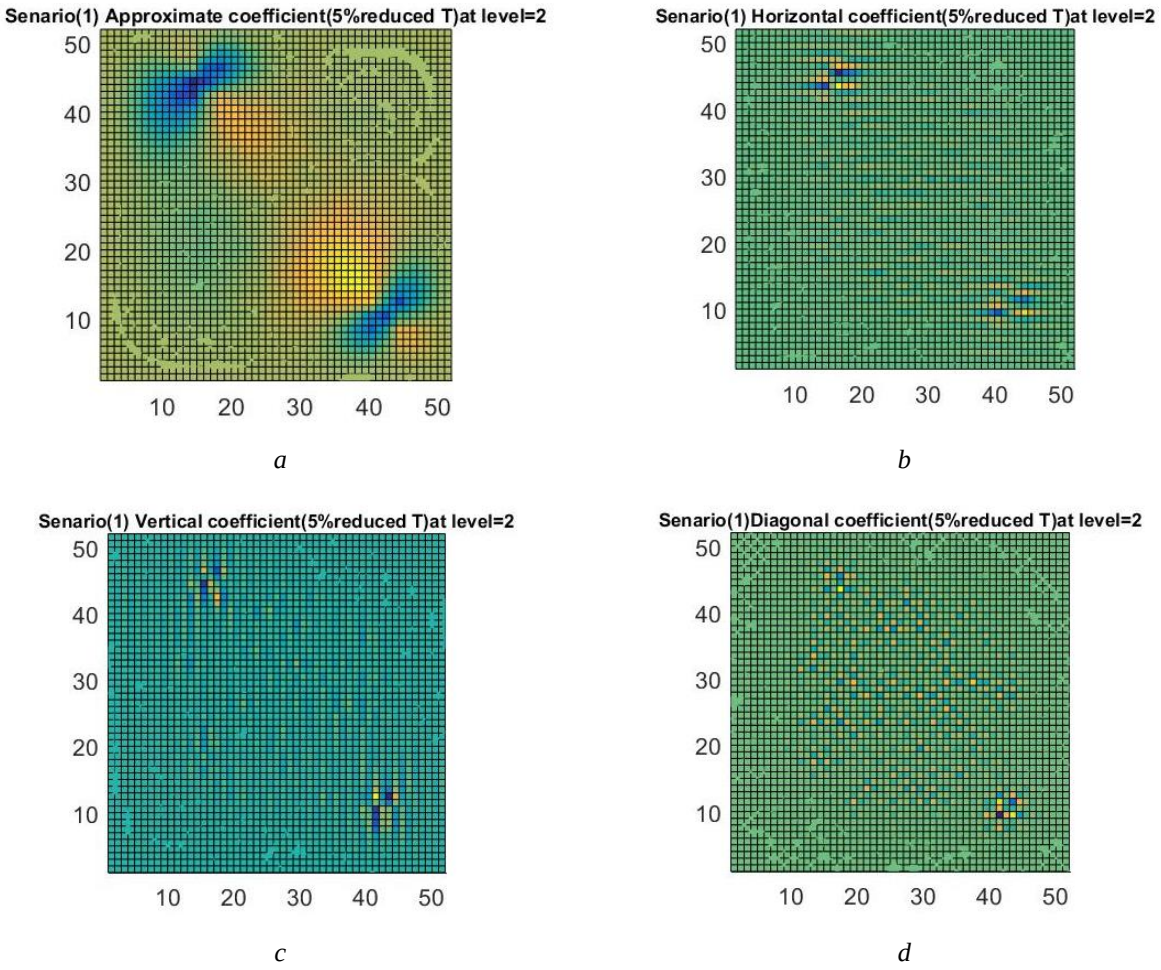

Figure 17: 2D Daubechies wavelet decomposition of scenario 1, at level 2 decomposition; a) approximation coefficients, b) Horizontal coefficients, c) Vertical coefficients, d) Diameter coefficients.

To investigate the application of two-dimensional curvelet transform for damage identification, Scenario 1 has been used by applying threshold and different scales from 3 to 5. The results are shown in Figure 18.

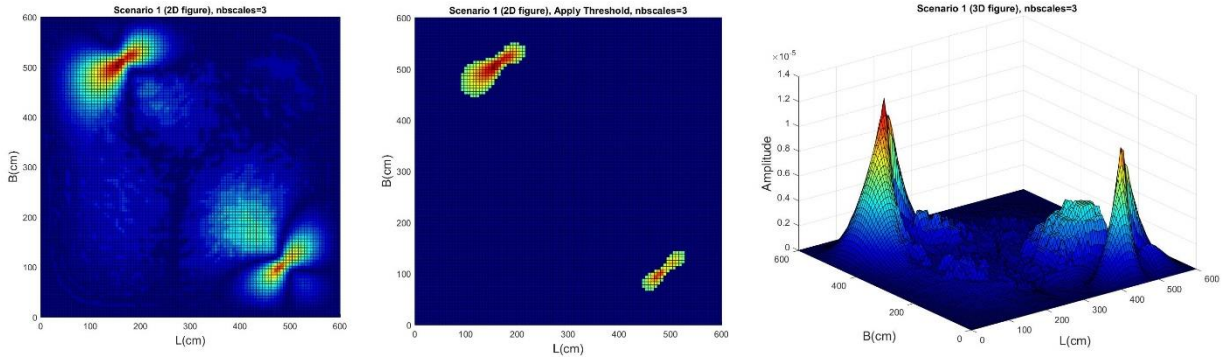

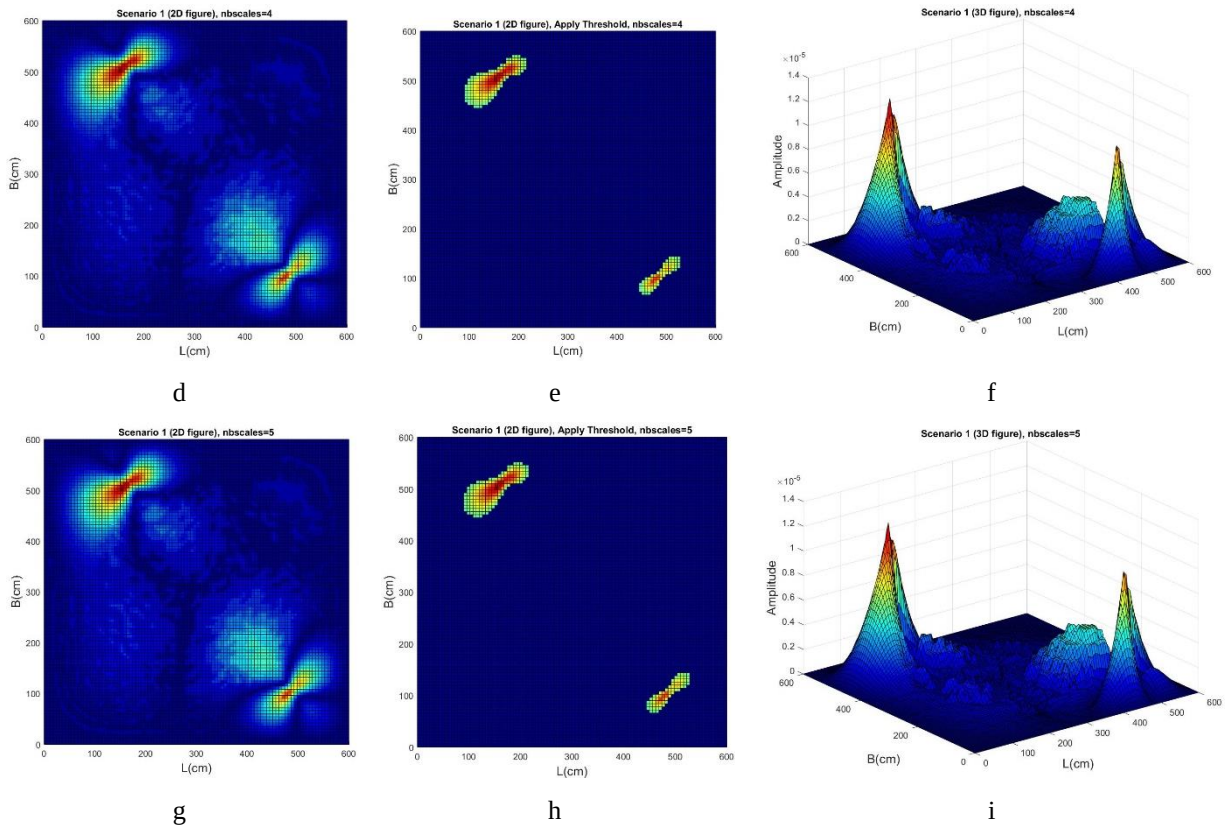

Figure 18: Two-dimensional curvelet transform of scenario 1 at nb_scale decomposition 3-5: a,c,f) 2D view of curvelet coffitions, b,d,g) apply threshold, and c,e,h) 3D view of curvelet coefficients of scale 3,4,5 respectively.

As shown in Figure 18, the damage's location is shown as a peak in the figures, and the location of the damage is exactly specified. Based on Figure 18(a, d, g) in three scales, scale=3,4 and 5 respectively, show the exact location of damaged area. Also, based on Figure 18(b, e, h), by applying the threshold, it can be seen that the location of the damaged area is clearer in terms of clarity compared to other cases, and this limitation makes the peaks of the location of damaged appear better. In Figure 18(c, f, i), the three-dimensional coefficients of the curvelet show the location of the damage better. As can be seen in Figure 18(c, f, i), the damaged area location larger corroding coefficients than the rest of the undamaged parts.

Scenario 2: Senario 2 is according to the previous scenario, however, a thickness reduction of 5% has been applied in one of the triangles.

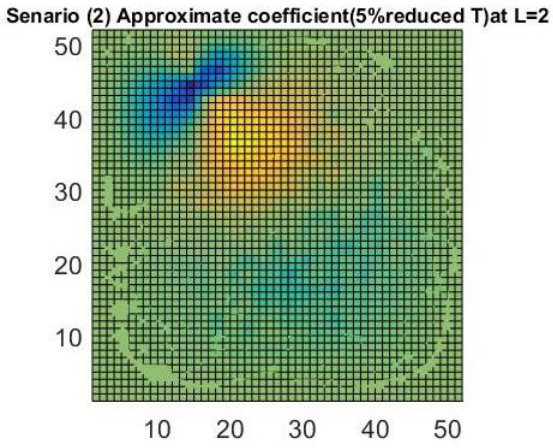
Senario (2) Approximate coefficient(5%reduced T)at L=2
50
40
30
20
10
10 20 30 40 50

a

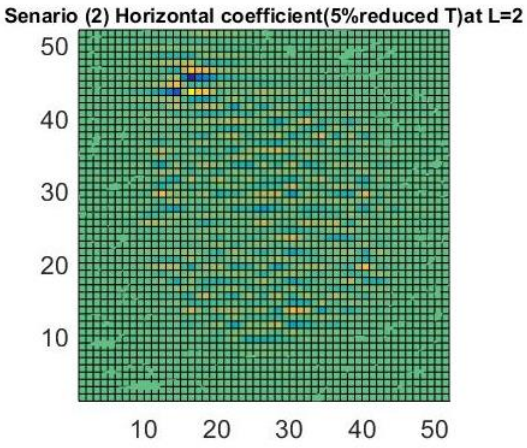
Senario (2) Horizontal coefficient(5%reduced T)at L=2
50
40
30
20
10
10 20 30 40 50

b

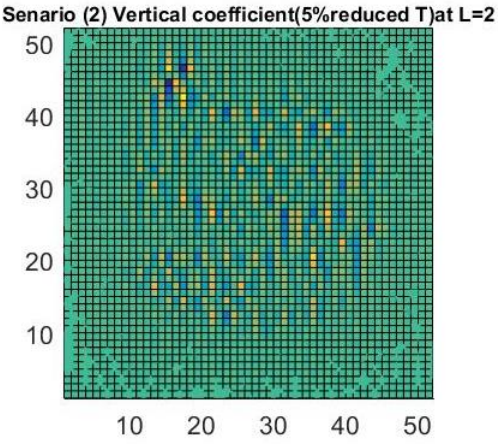
Senario (2) Vertical coefficient(5%reduced T)at L=2
50
40
30
20
10
10 20 30 40 50

c

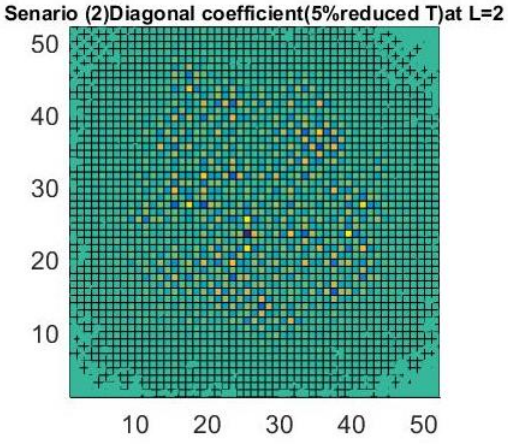
Senario (2)Diagonal coefficient(5%reduced T)at L=2
50
40
30
20
10
10 20 30 40 50

d

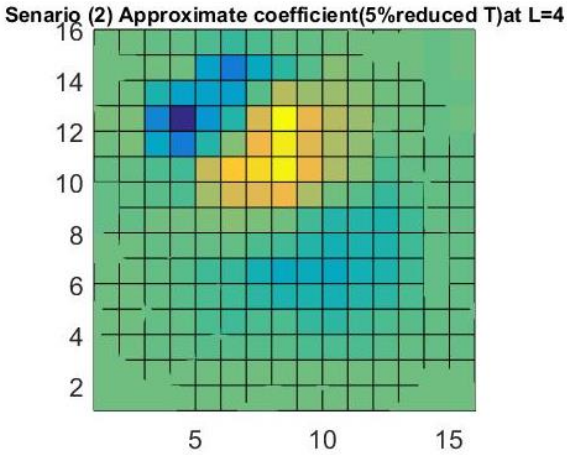
Senario (2) Approximate coefficient(5%reduced T)at L=4
16
14
12
10
8
6
4
2
5 10 15

e

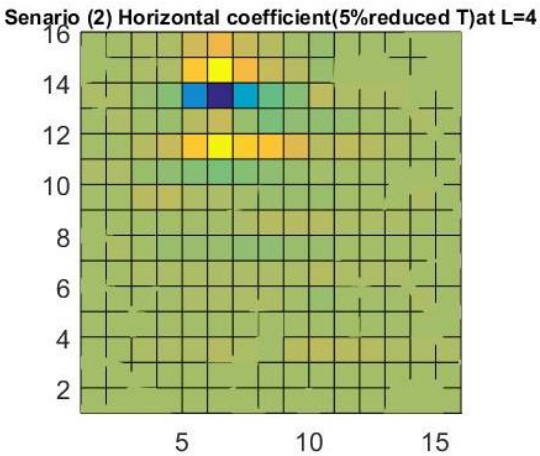
Senario (2) Horizontal coefficient(5%reduced T)at L=4
16
14
12
10
8
6
4
2
5 10 15

f

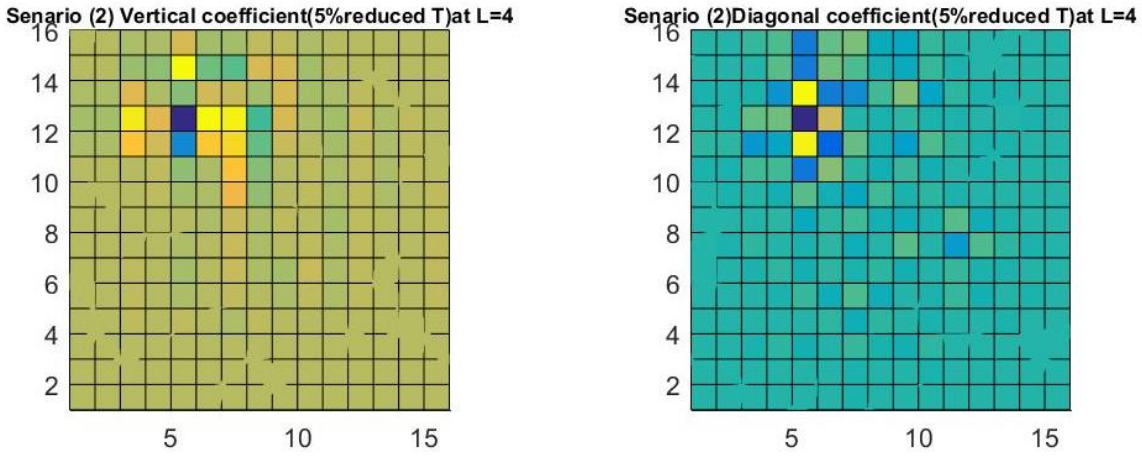

g h

Figure **19:** 2D Daubechies wavelet decomposition of scenario 2, at level 2 and 4 decomposition; a and e) approximation coefficients, b and f) Horizontal coefficients, c and g) Vertical coefficients, d and h) Diameter coefficients at level 2 and 4 decomposition, respectively.

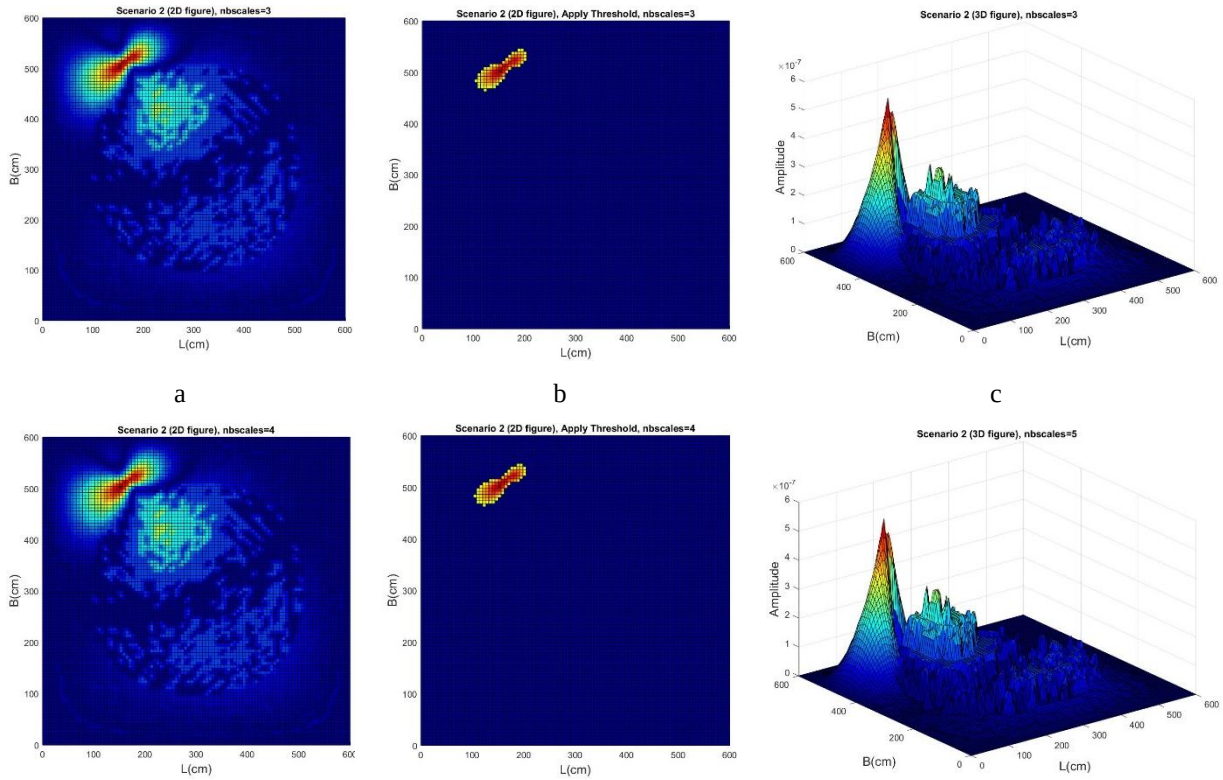

a b c

d e f

Figure **20:** Two-dimensional curvelet transform of scenario 2 at nb_scale=3 and 5 decomposition that; figure a and d) 2D view of curvelet coffitions, b and e) apply threshold, and c and f) 3D view of curvelet coefficients at scale 3 and 5, respectively.

Scenario 3: According to Figure 21, a square structure with dimensions of 500 cm in both directions, with a fixed support on all four sides and modulus of elasticity E = 20 GPa, mass density of ρ=2500 kg/m and Poisson's ratio ϑ = 0.3, and with 3 percent damage is considered.

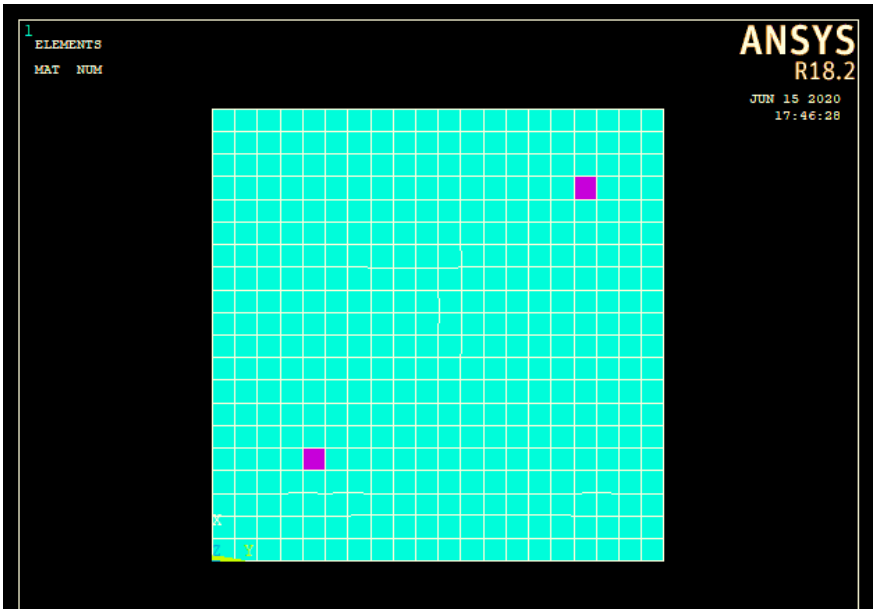

Figure 21: scenario 3, Geometry of the rectangle structure were considered rectangular damage with 3 percent reduced thickness.

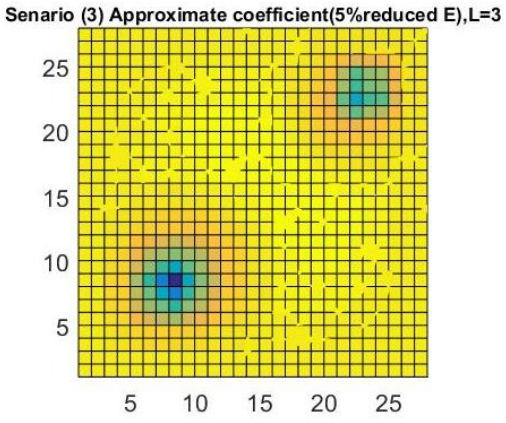

a

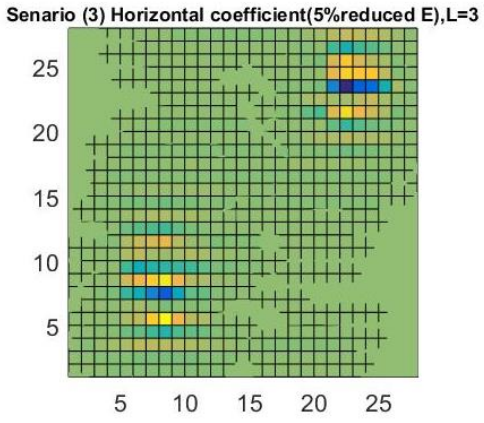

b

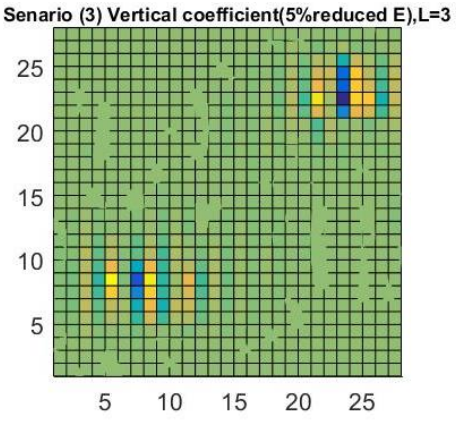

c

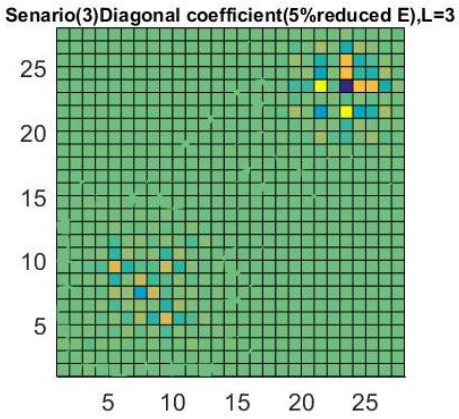

d

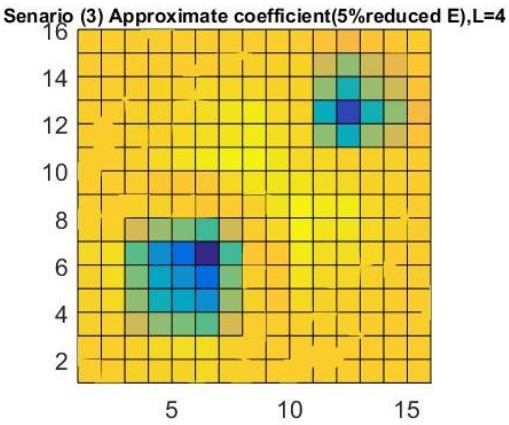

e

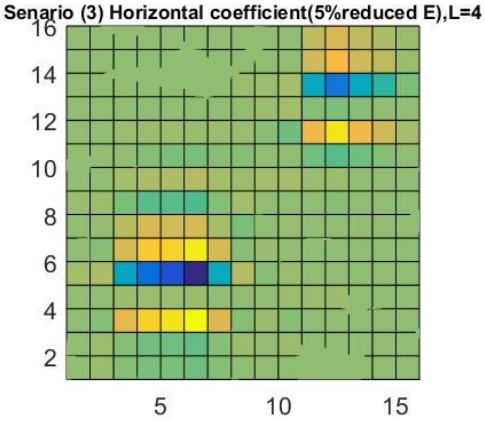

f

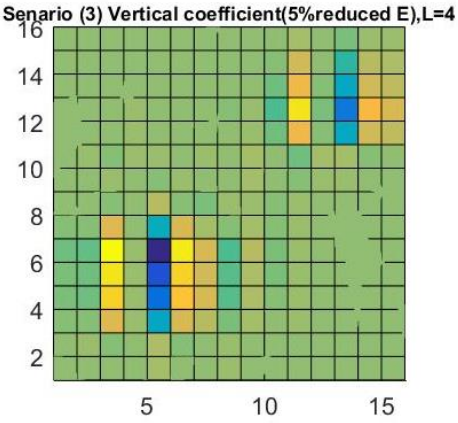

g

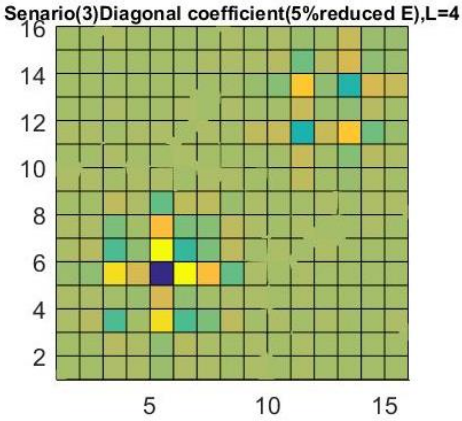

h

Figure **22:** 2D Daubechies wavelet decomposition of scenario 3, at level 3 and 4 decomposition; a,e) approximation coefficients, b, f) Horizontal coefficients, c, g) Vertical coefficients, d, h) Diameter coefficients for level 3 and 4 respectively.

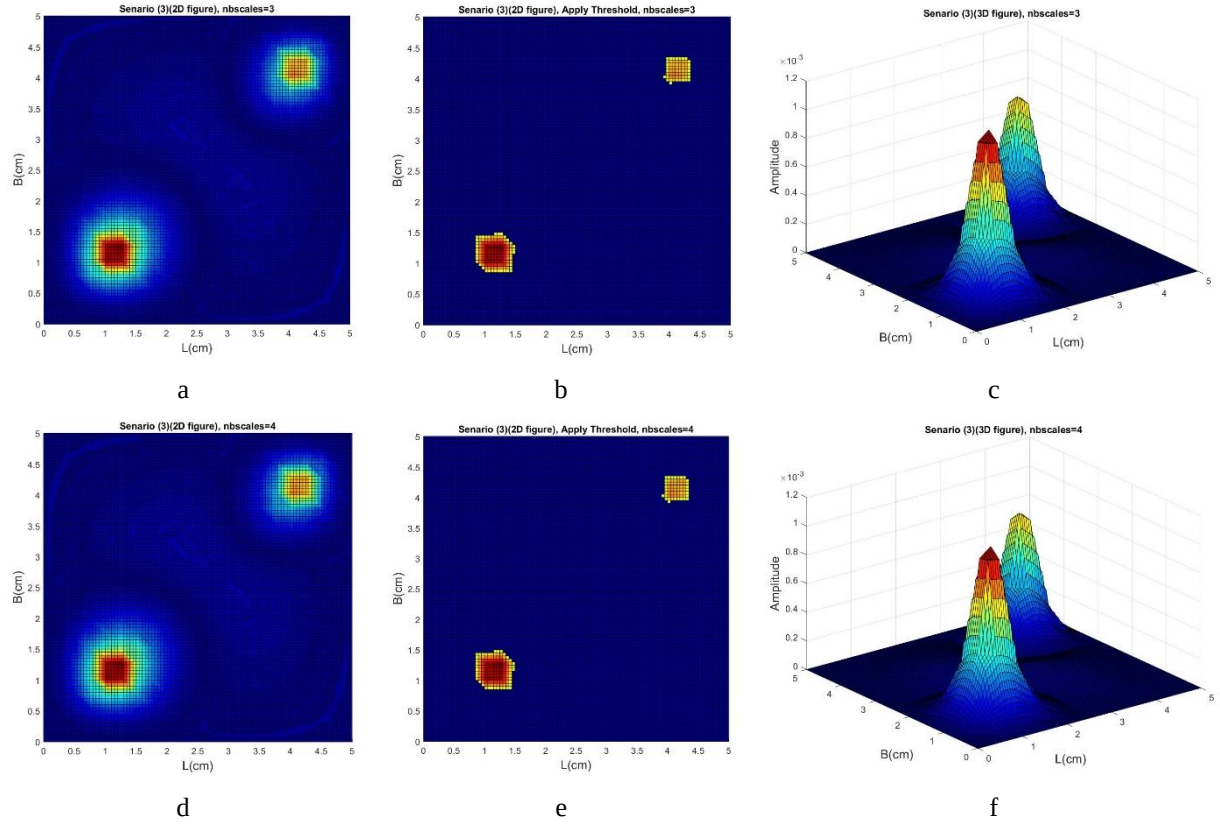

Figure **23:** Two-dimensional curvelet transform of scenario 3 at nb_scale=3 and 4 decomposition that; figure: a and d) 2D view of curvelet coffitions, b and e) apply threshold, and c and f) 3D view of curvelet coefficients at scale 3 and 4, respectively.

Scenario 4: According to Figure 24, a square dimension of 400 cm in both directions and a thickness of 20 mm, with fixed support on all four sides, modulus of elasticity of E = 20 GPa, mass density of ρ=2500 kg/m, Poisson's ratio $\vartheta = 0.3$, and with 3 percent damage is considered.

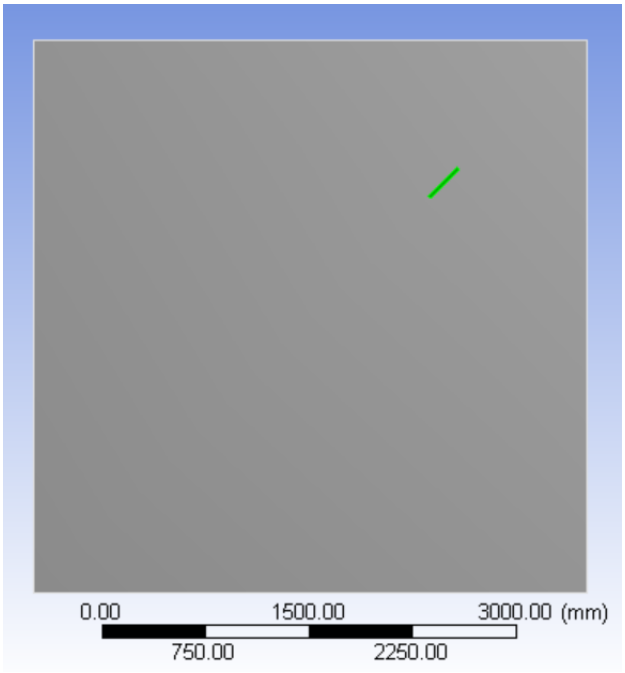

Figure 24: scenario 4, Geometry of the rectangle structure were considered rectangular damage with 3 percent reduced thickness.

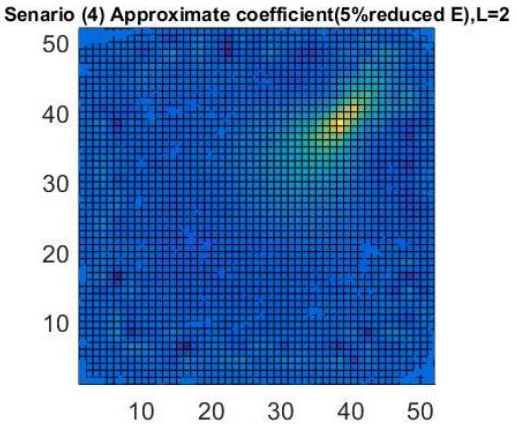

a

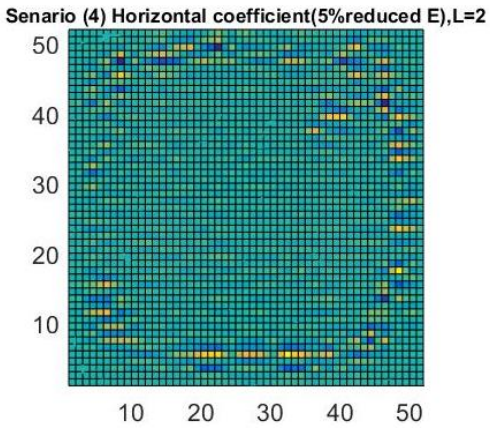

b

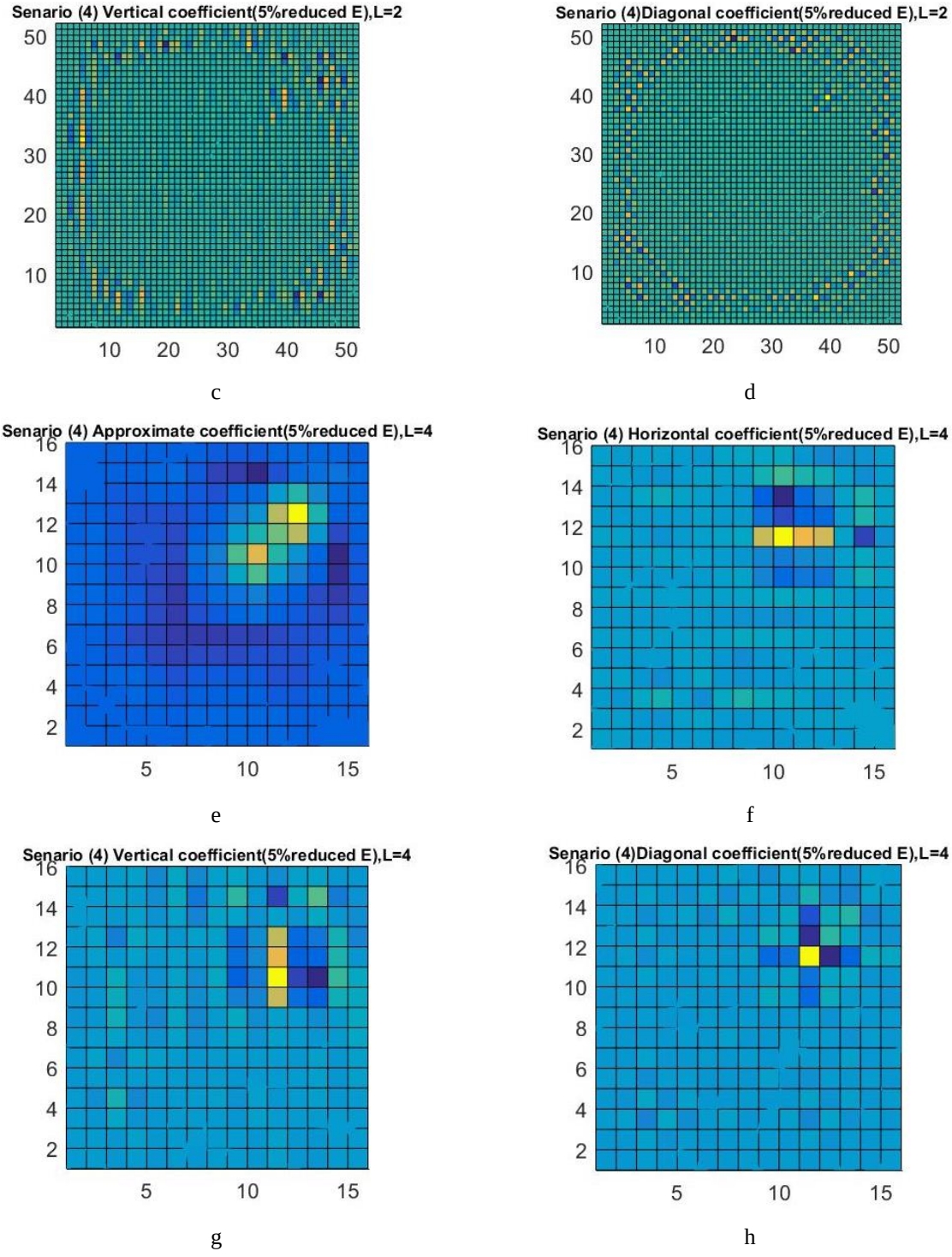

Figure 25: 2D Daubechies wavelet decomposition of scenario 4, at level 2 and 4 decomposition; a,e) approximation coefficients, b, f) Horizontal coefficients, c, g) Vertical coefficients, d, h) Diameter coefficients for decomposition level 2 and 4 respectively.

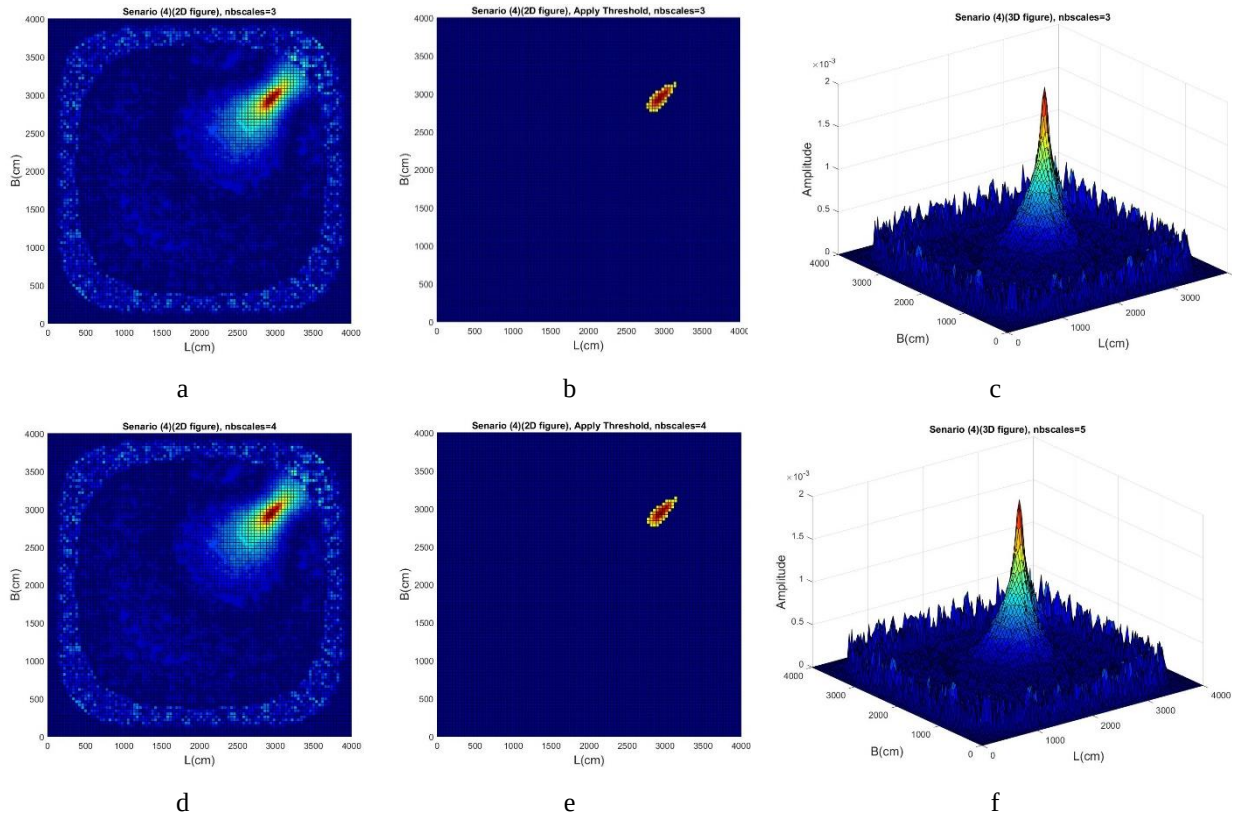

Figure **26:** Two-dimensional curvelet transform of scenario 4 at nb_scale=3 and 4 decomposition that; figure: a and d) 2D view of curvelet coffitions, b and e) apply threshold, and c and f) 3D view of curvelet coefficients at scale 3 and 4, respectively.

As shown in Figure 17 to Figure 26, the curvelet transform has a better ability than the wavelet transform to identify the location of damage with different percentages of damage, so the curvelet transform is recommended in identifying damage to two-dimensional structures due to its internal properties.

In order to investigate the application of contourlet transformation, 4 scenarios presented in the previous section have been examined by this converter. As shown in Figure 27 to Figure 30, this translation is able to correctly identify the location of damage.

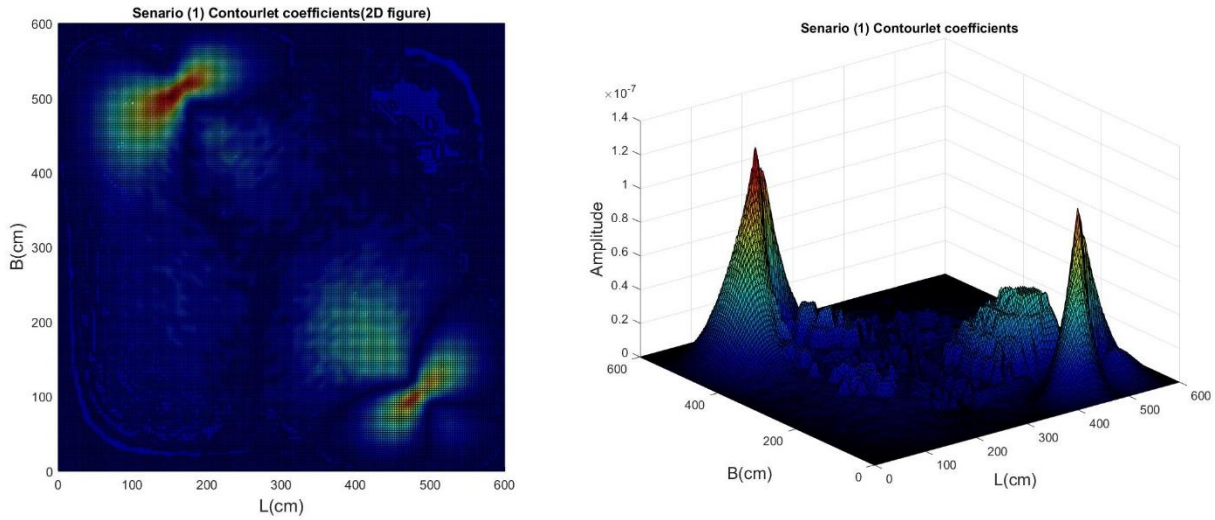

a b

Figure **27:** Damage detection of scenario 1, based on contourlet transform, a) 2D view of contourlet coefficients, b) 3D view of contourlet coefficients.

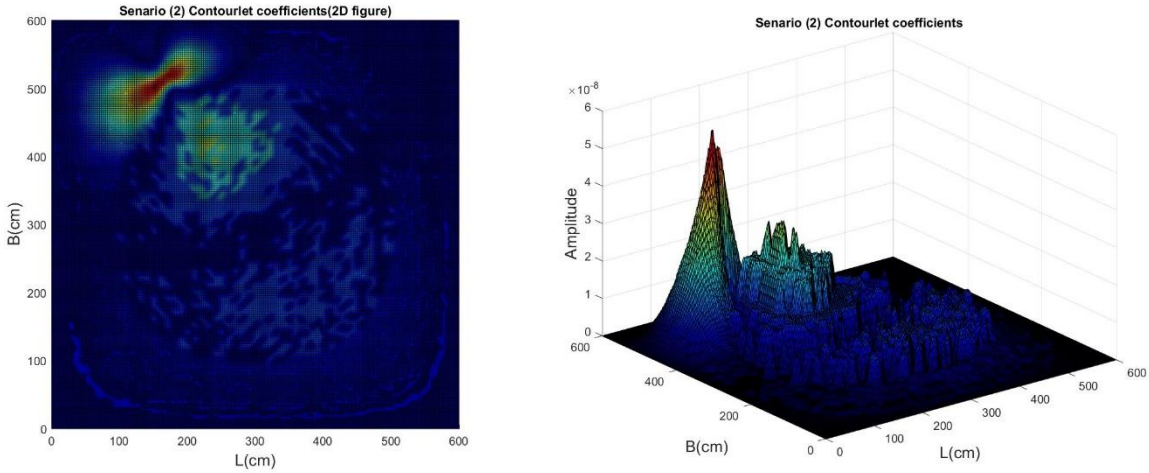

a b

Figure **28:** Damage detection of scenario 2, based on contourlet transform, a) 2D view of contourlet coefficients, b) 3D view of contourlet coefficients.

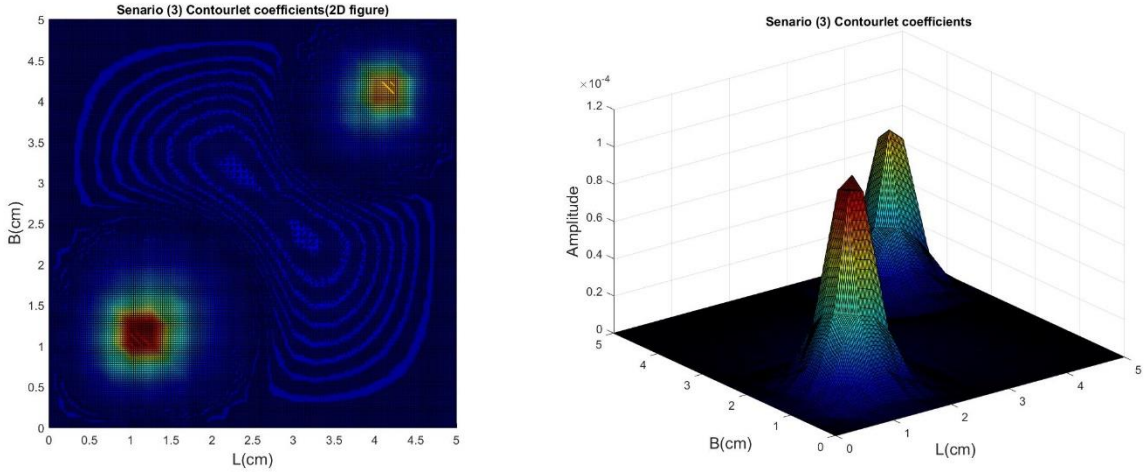

a b

Figure **29:** Damage detection of scenario 3, based on contourlet transform, a) 2D view of contourlet coefficients, b) 3D view of contourlet coefficients.

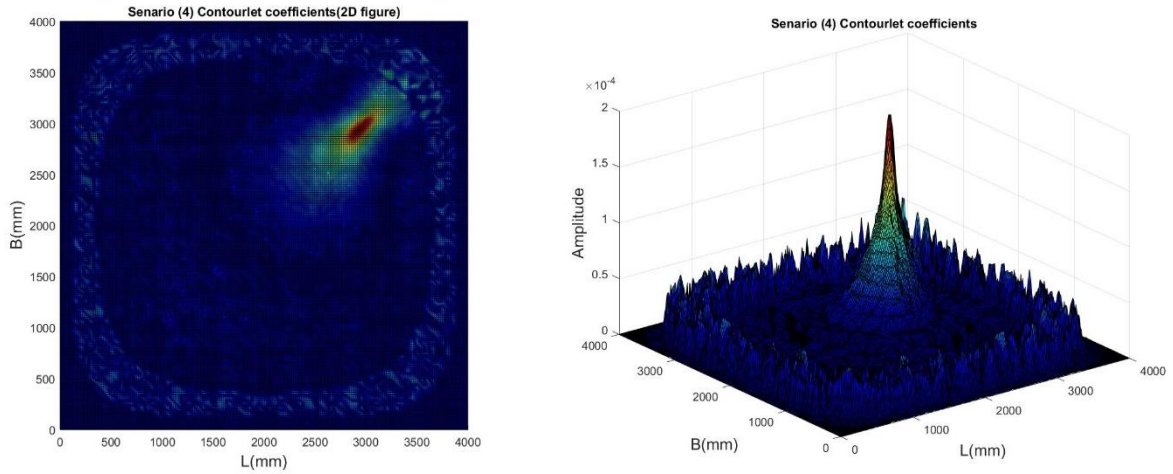

Figure **30:** Damage detection of scenario 4, based on contourlet transform, a) 2D view of contourlet coefficients, b) 3D view of contourlet coefficients.

6. Experimental validation study

In the previous section, the damage detection methods were evaluated based on numerical modeling for 4 scenarios. However, in order to evaluate the efficiency of the proposed methods, the efficiency of the above methods is examined based on laboratory data. In this section in accordance with an experimental data from the work of Rucka and Wilde [24], which is a steel plate with the specifications stated below.

According to Figure 31, a rectangle plate with dimension of L=560 mm and B=480mm, with thickness of 2 mm, with fixed support on all four sides, modulus of elasticity of E = 192 GPa, mass density of ρ=7850 kg/m^3, Poisson's ratio of $\vartheta = 0.25$, and with rectangle damage with 80m* 80mm and thickness 1.5 mm that equal to 25 percent damage in damaged area that located x=240 mm and y=240mm, considered.

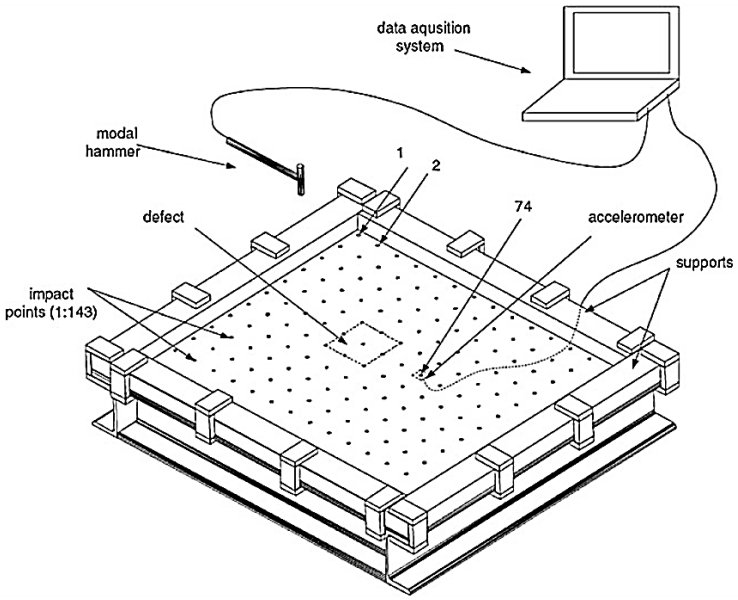

Figure 31: experimental steel plate based on Rucka and Wilde [24].

Based on the data extracted from the laboratory model, the above-mentioned transformations are used to troubleshoot the damaged structure, the results of which can be seen in the following figures. Due to the fact that the extracted data are accompanied by noise, for this purpose, the proposed method in section 5.2 has been used to add noise to the data.

Figure 32 shows the mode shape of the rectangle plate with noise and without noise. First, noise is applied to the input data, then the damaged transformation is applied to the data, and finally, using the threshold definition, the applied noise to the damaged transformation coefficients is removed. Figure 33 to Figure 35 show the results of wavelet, curvelet, and contourlet transformations. As can be seen, the transformation of contourlet and curvelet has more ability than the wavelet transforms in the detection of damage, and the contourlet against to curvelet has acted almost better and shows the location of the damaged with a better approximation. The results of this section confirm the results of numerical models in the 4 scenarios examined above.

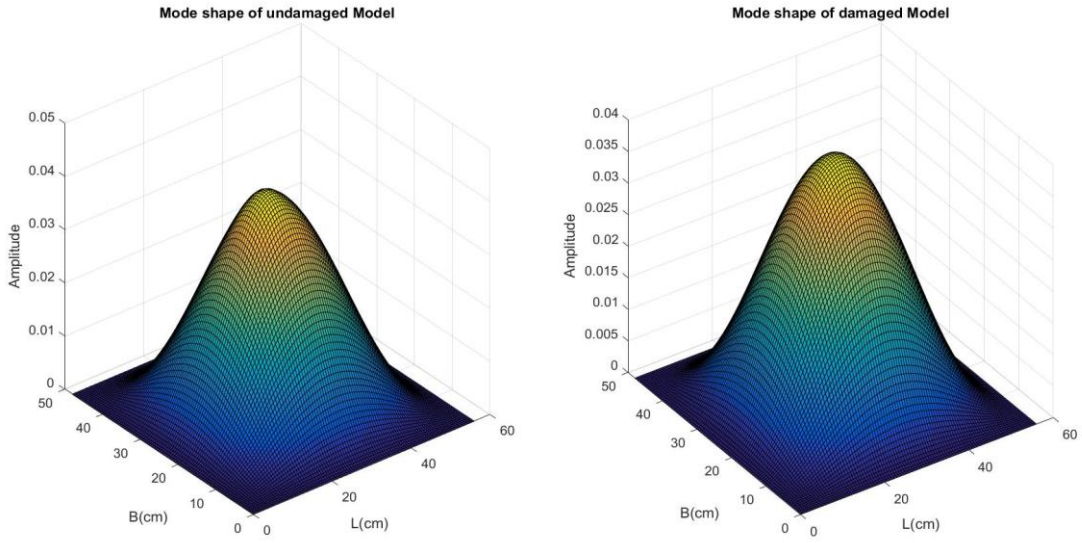

Figure 32: a) Experimental mode shape undamaged structure, b) mode shape of damaged model.

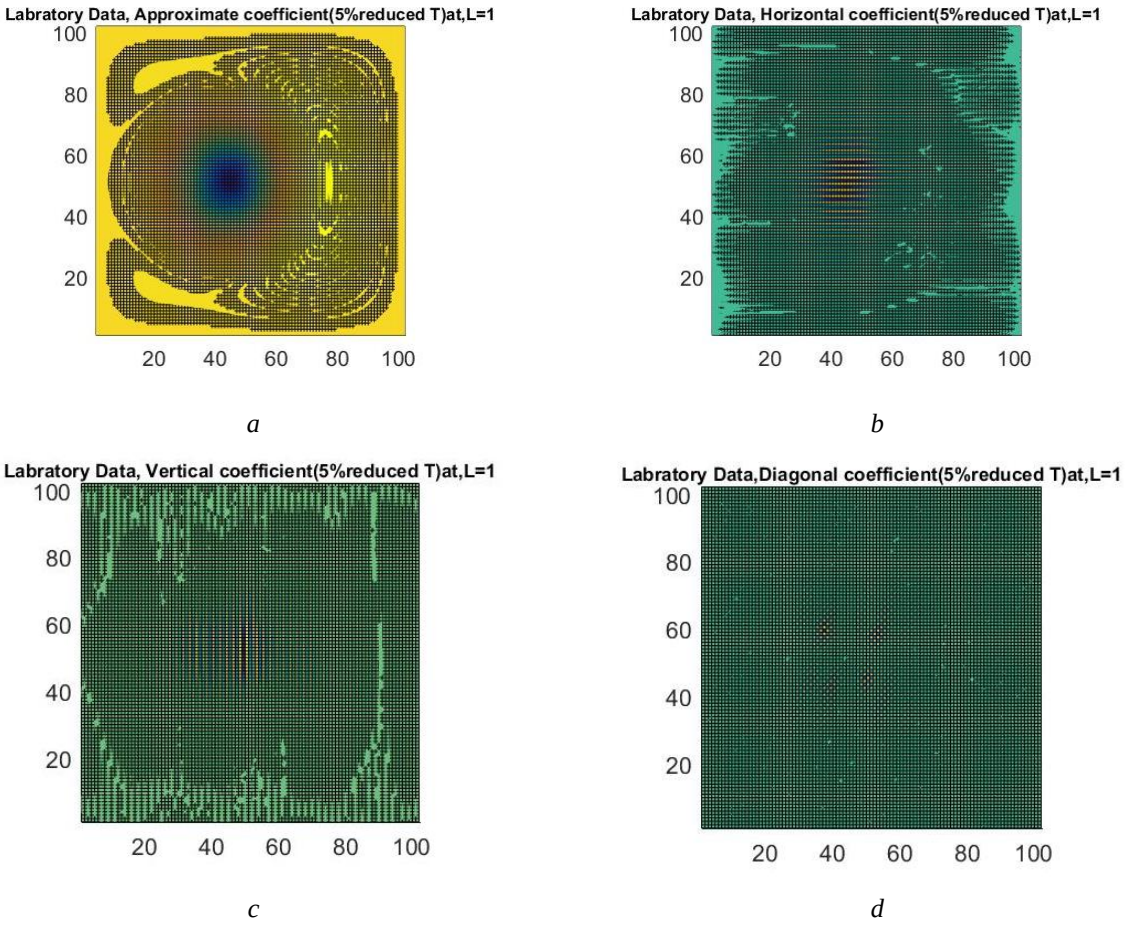

a *b*

c *d*

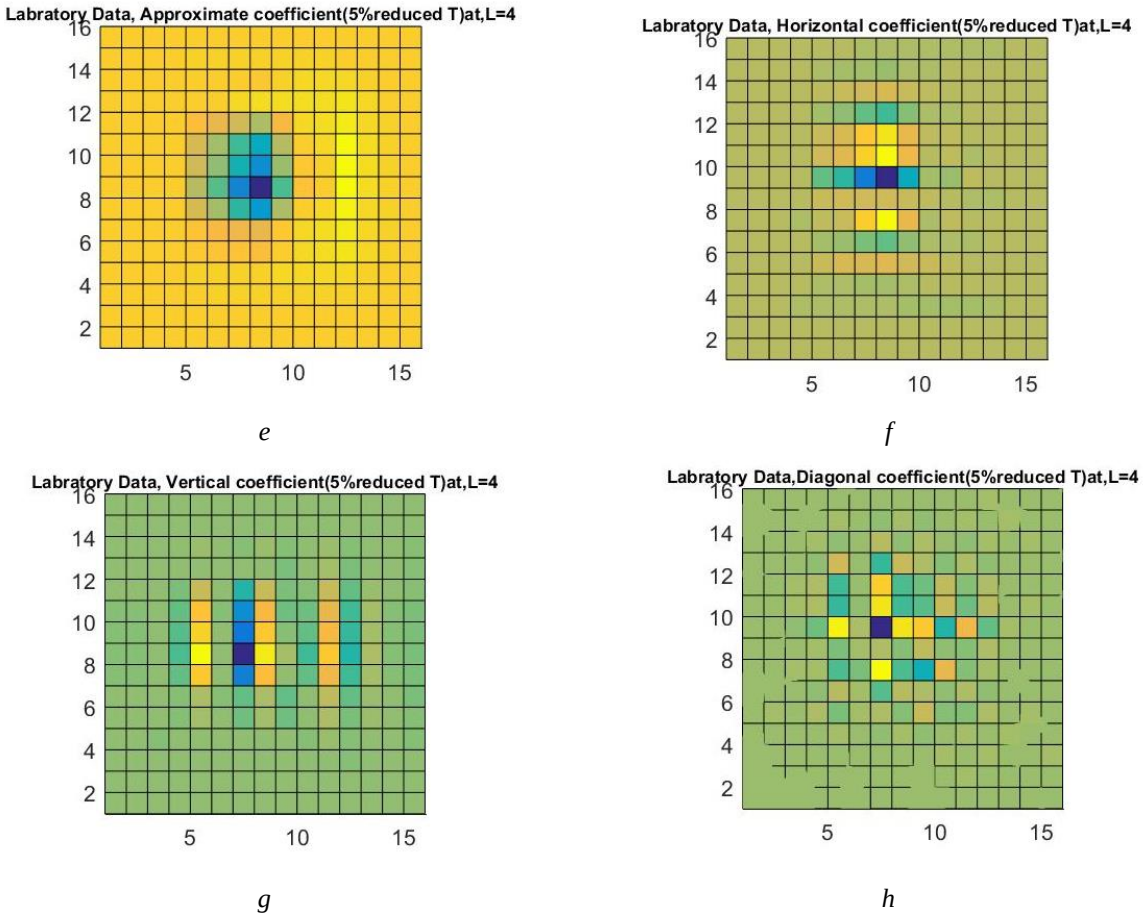

e *f*

g *h*

Figure 33: 2D Daubechies wavelet decomposition of Experimental data, at level 1 and 4 decomposition; a,e) approximation coefficients, b, f) Horizontal coefficients, c, g) Vertical coefficients, d, h) Diameter coefficients for decomposition level 1 and 4 respectively.

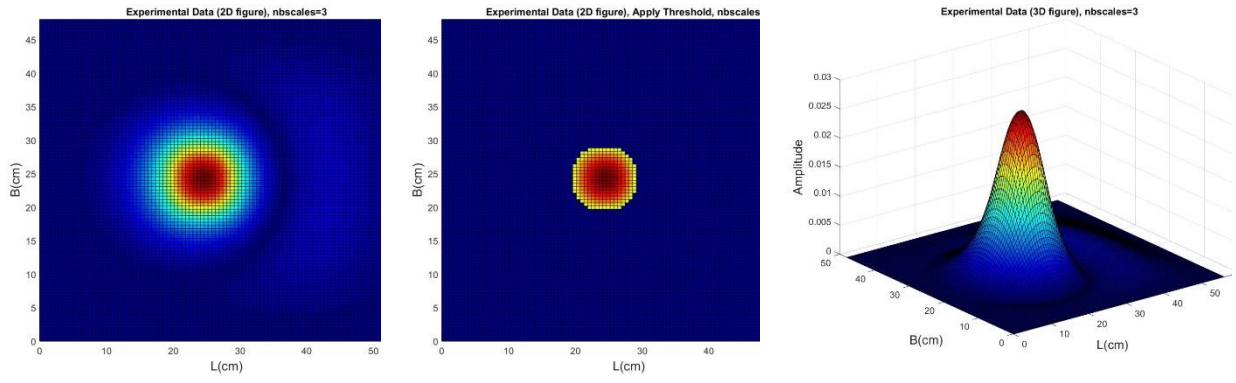

a b c

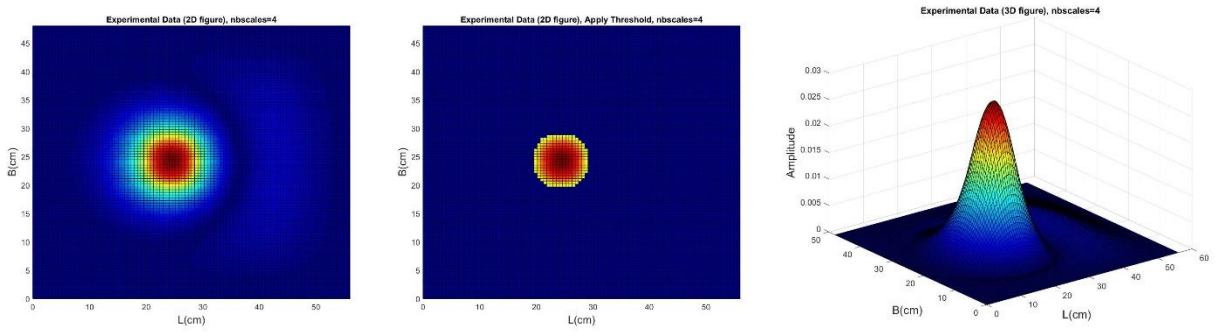

d e f

Figure **34:** Two-dimensional curvelet transform of experimental data at nb_scale=3 and 4 decomposition that; figure: a and d) 2D view of curvelet coffitions, b and e) apply threshold, and c and f) 3D view of curvelet coefficients at scale 3 and 4, respectively.

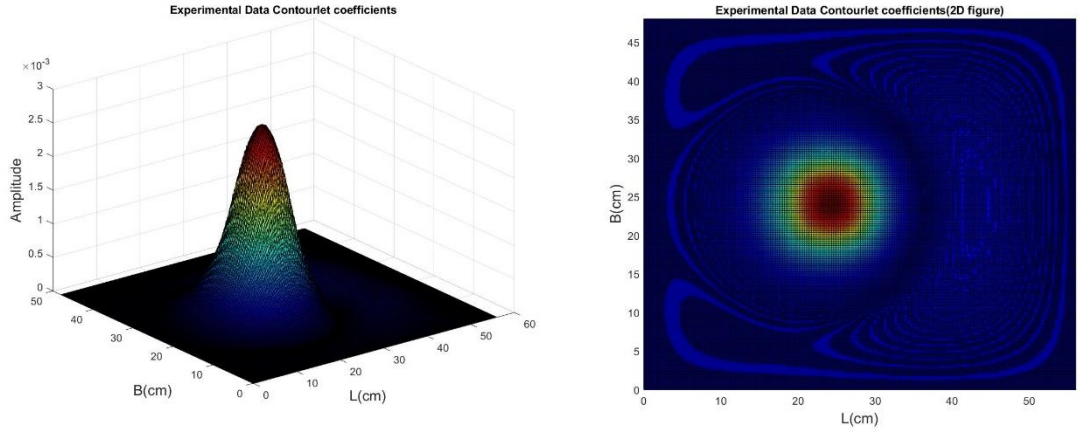

a b

Figure **35:** Damage detection of experimental plate based on Rucka and Wilde research data, a) 3D view of contourlet coefficients, b) 2D view of contourlet coefficients [24].

7. Conclusion

In this paper, three multi-scale transformations, including wavelet transforms, two-dimensional curvelet, and contourlet for fault detection in rectangular structures, were examined. To evaluate these transformations' performance, 4 scenarios with different locations, shapes, and percentage of damage were examined. Finally, laboratory results were used for a more detailed review. As the results show, the two-dimensional wavelet transform is weak in identifying the damage compared to the curvelet, and Contourlet transforms. The weakness of wavelet transform in damage detection is that the wavelet transform detects signals in one direction and cannot rotate. This translation is mostly used to identify one-way problems such as signals. Furthermore, the damage in different directions using two directional transformations of curvelet and contourlet has been identified. The curvelet and Contourlet transforms had a better display of a signal's details

due to their multi-scale and multi-directional nature. Because they were able to display details in all selected directions. The results show that both methods successfully identified the location of the damage. Still, in comparison with each other, the contourlet transform had more capability and almost better identified the damage's location.

:

References

[1] B. Asgarian, M. Amiri, and A. Ghafooripour, “Damage detection in jacket type offshore platforms using modal strain energy,” *Struct. Eng. Mech.*, vol. 33, no. 3, pp. 325–337, 2009.

[2] Z. Sun and C. C. Chang, “Vibration based structural health monitoring: Wavelet packet transform based solution,” *Struct. Infrastruct. Eng.*, vol. 3, no. 4, p. 0, 2007, doi: 10.1080/15732470500473598.

[3] J.-G. G. Han, W.-X. X. Ren, and Z.-S. S. Sun, “Wavelet packet based damage identification of beam structures,” *Int. J. Solids Struct.*, vol. 42, no. 26, pp. 6610–6627, 2005.

[4] D. Gabor, “Theory of communication,” *IEEE J.*, pp. 149–157, 1946.

[5] R. X. Gao and R. Yan, *Wavelets: Theory and Applications for Manufacturing*. Springer Verlag, 2010.

[6] R. R. Coifman and M. V Wickerhauser, “Entropy-based algorithms for best basis selection,” *Inf. Theory, IEEE Trans.*, vol. 38, no. 2, pp. 713–718, 2002.

[7] I. Daubechies, *Ten lectures on wavelets*. Society for Industrial Mathematics, 1992.

[8] E. Candes, D. L. Donoho, E. J. Candès, and D. L. Donoho, “Curvelets: A Surprisingly Effective Nonadaptive Representation of Objects with Edges,” *Curves Surf. Fitting*, vol. C, no. 2, pp. 1–10, 2000, [Online]. Available: http://citeseerx.ist.psu.edu/viewdoc/download?doi=10.1.1.34.2419&rep=rep1&type=ps%5Cnhttp://oai.dtic.mil/oai/oai?verb=getRecord&metadataPrefix=html&identifier=ADP011978%5Cnhttp://citeseerx.ist.psu.edu/viewdoc/summary?doi=10.1.1.43.6593.

[9] J. Ma and G. Plonka, “Computing with curvelets: From image processing to turbulent flows,” *Comput. Sci. Eng.*, vol. 11, no. 2, pp. 72–80, 2009, doi: 10.1109/MCSE.2009.26.

[10] J. Ma and G. Plonka, “A review of curvelets and recent applications,” *IEEE Signal Process. Mag.*, vol. 27, no. 2, pp. 118–133, 2010, [Online]. Available: https://www.uni-due.de/mathematik/plonka/pdfs/CurveletReviewshort.pdf.

[11] S. Shahverdi, M. A. Lotfollahi-Yaghin, and B. Asgarian, “Reduced wavelet component energy-based approach for damage detection of jacket type offshore platform,” *Smart Struct. Syst.*, vol. 11, no. 6, pp. 589–604, Jun. 2013, doi: 10.12989/sss.2013.11.6.589.

[12] M. A. Lotfollahi-Yaghin, S. Shahverdi, R. Tarinejad, and B. Asgarian, “Structural health monitoring (SHM) of offshore jacket platforms,” in *Proceedings of the International Conference on Offshore Mechanics and Arctic Engineering - OMAE*, 2011, vol. 1, doi: 10.1115/OMAE2011-49816.

[13] M. A. Lotfollahi-Yaghin and M. Koohdaragh, “Examining the function of wavelet packet transform (WPT) and continues wavelet transform (CWT) in recognizing the crack specification,” *KSCE J. Civ. Eng.*, vol. 15, no. 3, pp. 497–506, 2011.

[14] V. Karami, M. R. Chenaghlou, and A. R. M. Gharabaghi, “A combination of wavelet packet energy curvature difference and Richardson extrapolation for structural damage detection,” *Appl. Ocean Res.*, vol. 101, no. May, p. 102224, 2020, doi: 10.1016/j.apor.2020.102224.

[15] H. Doustmohammadi and A. Akbari Foroud, “A novel flicker detection method for vertical axis wind turbine using two-dimensional discrete wavelet transform,” *International Transactions on Electrical Energy Systems*. 2020, doi: 10.1002/2050-7038.12584.

[16] R. Nigam and S. K. Singh, “Crack detection in a beam using wavelet transform and photographic measurements,” *Structures*, vol. 25, no. March, pp. 436–447, 2020, doi: https://doi.org/10.1016/j.istruc.2020.03.010.

[17] G. Yan, Z. Duan, J. Ou, and A. De Stefano, “Structural damage detection using residual forces based on wavelet transform,” *Mech. Syst. Signal Process.*, vol. 24, no. 1, pp. 224–239, 2010, doi: 10.1016/j.ymssp.2009.05.013.

[18] M.-R. Ashory, A. Ghasemi-Ghalebahman, and M.-J. Kokabi, “Damage identification in composite laminates using a hybrid method with wavelet transform and finite element model updating,” *Proc. Inst. Mech. Eng. Part C J. Mech. Eng. Sci.*, vol. 232, no. 5, pp. 815–827, Feb. 2017, doi: 10.1177/0954406217692844.

[19] U. Poudel, G. Fu, and J. Ye, “Structural damage detection using digital video imaging technique and wavelet transformation,” *J. Sound Vib.*, vol. 286, no. 4–5, pp. 869–895, 2005, doi: 10.1016/j.jsv.2004.10.043.

[20] A. R. Hajizadeh, J. Salajegheh, and E. Salajegheh, “Performance evaluation of wavelet and curvelet transforms based-damage detection of defect types in plate structures,” *Struct. Eng. Mech. An Int. J.*, vol. 60, no. November25 2016, p. 15, 2016.

[21] A. Bagheri, G. Ghodrati Amiri, S. A. Seyed Razzaghi, G. G. Amiri, and S. A. S. Razzaghi, “Vibration-based damage identification of plate structures via curvelet transform,” *J. Sound Vib.*, vol. 327, no. 3–5, pp. 593–603, 2009, doi: 10.1016/j.jsv.2009.06.019.

[22] L. Ying, L. Demanet, and E. Candes, “3D discrete curvelet transform.”

[23] E. Candès *et al.*, “Fast discrete curvelet transforms,” *Multiscale Model. Simul.*, vol. 5, no. 3, pp. 861–899, 2006, doi: 10.1137/05064182x.

[24] M. Rucka and K. Wilde, “Crack identification using wavelets on experimental static deflection profiles,” *Eng. Struct.*, vol. 28, no. 2, pp. 279–288, 2006, doi: 10.1016/j.engstruct.2005.07.009.

[25] W. Bayissa, N. Haritos, and S. Thelandersson, “Vibration-based structural damage identification using wavelet transform,” *Mech. Syst. Signal Process.*, vol. 22, no. 5, pp. 1194–1215, 2008, doi: 10.1016/j.ymssp.2007.11.001.

[26] A. Shinde and Z. Hou, “A wavelet packet based sifting process and its application for structural health monitoring,” in *Structural Health Monitoring*, 2004, vol. 5, no. 2, p. 153.

[27] A. Ovanesova, “Applications of wavelet transforms to damage detection in frame structures,” *Eng. Struct.*, vol. 26, no. 1, pp. 39–49, 2004, doi: 10.1016/j.engstruct.2003.08.009.

[28] S. Shahverdi, M. A. Lotfollahi-Yaghin, M. H. Aminfar, and R. Valizadeh, “Damage detection in offshore free span pipelines using wavelet packet transform,” in *Proceedings of the International Conference on Offshore Mechanics and Arctic Engineering - OMAE*, 2011, vol. 4, doi: 10.1115/OMAE2011-49803.

[29] X. Jiang, S. Mahadevan, and H. Adeli, “Bayesian wavelet packet denoising for structural system identification,” *Struct. Control Heal. Monit.*, vol. 14, no. 2, pp. 333–356, Mar. 2007, doi: 10.1002/stc.161.

[30] E. J. Candès and L. Demanet, “The curvelet representation of wave propagators is optimally sparse,” *Commun. Pure Appl. Math.*, vol. 58, no. 11, pp. 1472–1528, Nov. 2005, doi: 10.1002/cpa.20078.